TCF-1 in CD8 T cells separates GVHD from GVL

Rebecca Harris[1], Mahinbanu Mammadli[1], Adriana May[1], Qi Yang[2], Ivan Ting Hin Fung[2], Jyoti Misra Sen[3,4], Mobin Karimi[1*]

[1]Department of Microbiology and Immunology, SUNY Upstate Medical University, Syracuse, NY 13210.
[2]Department of Immunology and Microbial Disease, Albany Medical College, Albany, NY 12208
[3]National Institute on Aging-National Institutes of Health, 08C218,Biomedical Research Center, 251 Bayview Boulevard, Suite 100, Baltimore, MD 21224
[4]Immunology Program, Department of Medicine, Johns Hopkins School of Medicine, Baltimore, MD 21224.

To whom correspondence should be addressed:
Mobin Karimi
Assistant Professor of Immunology and Microbiology
SUNY Upstate Medical University,
766 Irving Ave Weiskotten Hall Suite 2281,
Syracuse, NY 13210
Office Phone: 315-464-2344
Laboratory Phone: 315-464-7652
Email: karimim@upstate.edu

Conflict of interest statement: The authors have declared that no conflict of interest exists

Abstract

Allogeneic hematopoietic stem cell transplantation (allo-HSCT) is a curative treatment for hematological malignancy due to graft-versus-leukemia (GVL) effects, mediated by alloreactive donor T cells. However, these same donor cells cause graft-versus-host disease (GVHD), a life-threatening complication. During GVHD, donor T cells proliferate, migrate, and produce cytokines, leading to damage of healthy host tissues. Separating the linked processes of GVHD and GVL is critical to improving outcomes. Here we show that TCF-1, a major T cell developmental factor, plays a role in regulation of these processes. Using a mouse model of allo-HSCT leading to GVHD, we found that conditional loss of TCF-1 in mature CD8 T cells separates GVHD from GVL, providing an optimal clinical phenotype. This occurred due to changes in cytokine production, proliferation, cell survival, chemokine receptor expression, and gene expression. Thus, modulation of TCF-1 signaling reduces GVHD severity and persistence, but maintains GVL effects, and could be useful for allo-HSCT or other T cell-mediated disorders. Furthermore, here and in our companion manuscript we show that regulation of mature, alloactivated T cells by TCF-1 differs between CD4 and CD8 T cells, suggesting that TCF-1 is critical for regulation of mature alloactivated T cells, with unique programs in each subset.

Introduction

Allogeneic hematopoietic stem cell transplantation (allo-HSCT) is a curative therapy often used for hematological malignancies (1). Mature donor T cells found in the graft become alloactivated upon recognition of host HLA as non-self (2, 3). This leads to T cell proliferation, migration to target organs, and cytokine production(4) These T cell activities help to clear residual malignant cells, which is called the graft-versus-leukemia effect (GVL)(5) (6). However, 30 to 70 percent of patients also experience graft-versus-host disease (GHVD), a serious complication driven by the same mature donor T cells (6). Damage to healthy host tissues during GVHD is a major problem for widespread use of allo-HSCT (7-9).Our work and that of others focuses on modulating donor T cell signaling to separate the linked processes of GHVD and GVL (9-11). In this manuscript, as well as in our companion manuscript, we address the role of T Cell Factor-1 (TCF-1), a major T cell developmental transcription factor, in regulating these processes(12) TCF-1 is involved in the Wnt signaling pathway, and is critical for T cell development as well as activation (12-14) . However, it in unknown whether TCF-1 also regulates mature alloactivated T cells, and whether modulation of this factor may affect GVHD or GVL. TCF-1 has been reported to control Eomesodermin (Eomes) and possibly T-box transcription factor 21 (T-bet), two downstream transcription factors which are known to be involved in GVHD and GVL (10, 15, 16). Therefore, we hypothesized that TCF-1 may also affect and possibly separate these processes.

Using a mouse model of GVHD and GVL following allo-HSCT, we were able to study all of the major T cell functions, as well as phenotypes, clinical outcomes, and gene expression, in a single model. We also used a unique mouse strain which has deletion of TCF-1 in mature T cells, rather than a global deletion (17). This Tcf7 flox/flox x CD4cre mouse experiences

deletion of TCF-1 in all T cells at the double-positive phase of development, when all T cells express CD4 (17). This allows us to overcome the severe T cell developmental defect that occurs in global TCF-1 deletion, as TCF-1 is critical for the double-negative stage of development (17) . Using these tools, we found that loss of TCF-1 reduces both the severity and the persistence of CD8 T cell-driven GVHD, but maintains GVL functionality of mature alloactivated CD8 T cells. For GVHD reduction, this is primarily due to reduced cytokine production, increased predisposition to apoptosis, increased exhaustion, and possibly reduced proliferation of alloactivated donor T cells, as well as increased central memory cells at baseline (18-20). GVL effects are maintained against liquid tumors, due to increased donor T cell activation and production of the cytotoxic mediators perforin and Granzyme B (21, 22). We showed that loss of TCF-1 induces T cell-intrinsic phenotypic changes which promote GVL effects while disrupting GVHD, including increased expression of Eomes, T-bet, CD122, CD44, and CD8 central memory. The frequency of activating/transitioning CD8 T cells dropped when TCF-1 was lost. Loss of TCF-1 affected expression of chemokine receptors on donor T cells, which was previously unknown (18).

TCF-1 loss also affected pathways for T cell differentiation, cell adhesion, signaling (MAPK, NFkB, calcium, TCR, NOD, TNF, and others), cell cycle, necroptosis, cell senescence, autophagy, metabolism, and DNA replication (22).

Recent reports have identified a novel subset of CD8+ T cells which express CXCR5, a marker traditionally associated with T follicular helper cells (23) . These CXCR5+ CD8+ T cells are thought to be stem-like, and help to maintain pools of CD8 T cells during chronic responses to antigen (24). These cells have been described in situations where antigen is persistently present, such as chronic infections (25). We hypothesized that these cells may also play a role in

GVHD, where damaging disease persists over time, and exposure to alloantigen in the host is chronic (26). Indeed, we found that CXCR5+ CD8+ T cells are present in mice experiencing GVHD from WT CD8+ T cells. The peak frequency of these cells correlated temporally with peak clinical score. Additionally, mice given TCF cKO CD8+ T cells had lower frequencies of donor-derived CXCR5+ CD8+ T cells, suggesting that these cells may be important for sustaining GVHD responses over time.

Therefore, TCF-1 controls mature CD8 T cell phenotype and functions during alloactivation, a novel finding. Together with our companion paper, we have shown that regulation of mature alloactivated CD4 versus CD8 T cells by TCF-1 is different. Modulation of TCF-1 and Wnt signaling may be a successful option for separating GVHD from GVL to improve patient outcomes following allo-HSCT. We also identified a role for CXCR5+ CD8+ T cells in GVHD, providing another potential target for T cell modulation to improve patient outcomes.

Results

Loss of TCF-1 in donor CD8 T cells reduces severity and persistence of GVHD symptoms.

Most of the previous research on TCF-1 utilized a global TCF-1 knockout, because the primary focus was on TCF-1's role as a developmental factor. However, we wanted to study the role of TCF-1 in mature T cells. Global loss of TCF-1 results in minimal T cell production from the thymus, because TCF-1 is critical for DN stages of development. Therefore, we obtained mice with a T cell-specific knockout for TCF-1 (Tcf7 flox/flox x CD4cre, called TCF cKO here (17). This allowed us to study mature T cells that developed normally in the thymus, then lost expression of TCF-1 at the DP phase.

To determine whether TCF-1 plays a role in mature alloactivated T cell regulation, which is currently unknown, we used a mouse model of MHC-mismatched allo-HSCT leading to GVHD and GVL. Briefly, BALB/c mice (MHC haplotype d) were lethally irradiated and transplanted with BALB/c bone marrow and C57Bl/6-background (MHC haplotype b) donor CD8 T cells (10). The donor cells came from wild-type (WT), CD4cre-positive (CD4cre), or TCF-1-deficient (TCF cKO) mice. Recipients were given $1X10^6$ CD8 T cells and $10X10^6$ BALB/c T cell-depleted bone marrow cells, as well as $2X10^5$ B-cell acute lymphoblastic leukemia (B-ALL) tumor cells (27) to assess GVL responses (10). B-ALL is syngeneic to BALB/c mice and allogeneic to C57BL/6 (B6) mice (10). The MHC haplotype mismatch between host and donor cells drives alloactivation of donor T cells, which in turn causes GVHD and GVL effects. To examine disease severity and progression, recipient mice were weighed and given a clinical score three times per week following transplant, until about day 60 **(Fig. 1A)**. The mice were scored based on six factors: skin integrity, fur texture, posture, activity level, weight loss, and diarrhea (28) .

We found that mice who received WT donor T cells had a rapid increase in GVHD severity, with a high peak score around day 7, suggesting severe GVHD **(Fig. 1A)**. This high score was maintained until the recipient mice died of disease, suggesting persistent disease **(Fig. 1A)**. Disease burden, as determined by the percent of mice in each group that died during the experiment, was high for WT-transplanted mice **(Fig. 1B)**. WT-transplanted mice lost weight initially, and were unable to regain much weight (**Supp. Fig. 1A)**. Most mice that received WT T cells also died prior to day 60 **(Fig. 1A-C)**. Recipient mice given CD4cre T cells showed no significant differences in survival or clinical score from those given WT T cells **(Fig. 1A-C), (Supp. Fig. 1A)**. In contrast, mice given TCF cKO T cells had much better survival, lower peak and average clinical scores, lower disease burden, and a gain in weight following the initial weight loss period **(Fig.1A-C), (Supp. Fig. 1A)**. In addition, the clinical scores for these mice quickly reduced to near-control levels following peak score at day 7 **(Fig. 1A)**, suggesting that disease does not persist in these mice. Therefore, loss of TCF-1 in donor T cells led to reduced GVHD severity and persistence, with improved survival.

During GVHD, host tissues are damaged by the activity of alloactivated T cells. To determine whether damage to target organs of GVHD (skin, liver, and small intestine AKA "gut") was altered by loss of TCF-1 in donor T cells, we collected organs from mice allotransplanted as described above. At day 7, day 14, and day 21 post-transplant, we collected pieces of skin, small intestine, and liver from recipient BALB/c mice. These organs were fixed, sectioned, stained with hematoxylin and eosin (H&E), and scored by a pathologist (A.M.) blinded to study group and donor type **(Fig. 1D)**. At day 7, there is little to no difference observed between WT- and TCF cKO-transplanted organs, except for a trend toward reduced median grade in the gut for TCF cKO-transplanted mice **(Supp. Fig. 1B)**. This correlates with

the observation that until day 7, disease course appears similar in both groups, with a decreased peak score appearing at day 7 **(Fig. 1A)**. By day 21, significant differences in the number of mice per group with severe versus mild GVHD grades (3-4 for severe versus 0-2 for none to moderate)(29)(30) for the liver and skin were observed, with WT-transplanted mice having more severe disease **(Fig. 1E)**. In addition, the median grade for all organs trended towards decreased for TCF cKO-transplanted mice, which correlated with the lymphocyte infiltration and tissue damage seen in slide photos **(Supp. Fig. 1B-C)**. These changes were already visible by day 14 as a trend, suggesting that TCF cKO-transplanted mice have altered disease course after peak score at day 7 **(Supp. Fig. 1B-C)**. Altogether, these data suggest that TCF-1 normally promotes GVHD damage to healthy tissues, and is indispensable for T cells to cause this damage. Thus, loss of TCF-1 in donor T cells leads to reduced severity and persistence of GVHD over time.

TCF-1-deficient CD8 T cells retain anti-tumor capabilities for the graft-versus-leukemia (GVL) effect. We showed that TCF-1-deficient donor T cells reduce the severity and persistence and GVHD. However, it is clinically optimal if GVL effects are maintained despite reduced GVHD, because the same donor T cells mediate both effects. Therefore, we tested whether GVL effects were compromised by loss of TCF-1 in donor T cells. We used the allo-HSCT mouse model described in Fig. 1 to assess GVL responses. The B-ALL cells expressed luciferase (10), allowing us to track them by injecting D-luciferin into the recipient mice, and imaging them with an *in vivo* bioluminescence scanner (IVIS 200). The mice were weighed, scored, and scanned three times a week until the end of the experiment **(Fig. 2)**.

At day 1 post-transplant, recipient mice from all groups (B-ALL luc+BM only, B-ALL luc+BM+WT CD8 T cells, B-ALL luc +BM+TCF cKO CD8 T cells, and B-ALL luc

+BM+CD4cre CD8 T cells) showed detectable levels of tumor cells in their bodies **(Fig. 2A)**. $2X10^5$ tumor cells were injected, so they were immediately detectable, but not overwhelming for the donor T cells(10). Over time, the group receiving only bone marrow and tumor cells showed a large increase in tumor growth **(Fig. 2A-B)**, because no T cells were present to control the tumor cells. In contrast, most mice given CD8 T cells from any donor type along with the BM and B-ALL luc cells were able to clear the tumor cells by the end of the experiment **(Fig. 2A-B)**. The GVL effect was maintained even in CD4cre and TCF cKO-transplanted mice, with little difference in quantified bioluminescence between groups **(Fig. 2B)**. Tumor burden was also similar between WT and TCF cKO-transplanted mice **(Fig. 2C)**. As seen before in Fig 1, mice in the WT and CD4cre groups died from GVHD over time, but mice in the TCF cKO group had mild GVHD that resolved over time **(Fig. 1A,2A)**. Altogether, these data show that TCF-1 is dispensable for GVL effects, but critical for GVHD. Therefore, loss of TCF-1 in donor T cells provides a clinically optimal phenotype, where GVHD severity is reduced but beneficial GVL effects are maintained.

Loss of TCF-1 drives changes to mature CD8 T cell phenotype which are primarily cell-intrinsic. Alloactivated T cells must survive, proliferate, produce cytokines, and migrate to target organs in order to mediate GVHD or GVL. The phenotype of the donor T cell can also affect its ability to perform these functions and contribute to GVHD/GVL. To determine whether loss of TCF-1 affected mature donor T cell phenotype, we performed flow cytometry phenotyping on pre-transplant donor CD8 T cells **(Fig. 3A-E)**. To begin, we looked at expression of Eomesodermin (Eomes) and T-box transcription factor 21 (T-bet), both of which are downstream of TCF-1. Eomes and T-bet both are known to contribute to GVHD, and Eomes is also critical

for GVL effects (10, 31). Some reports have claimed that Eomes is activated by TCF-1 (meaning loss of TCF-1 reduces Eomes expression (15). However, in our model of conditional TCF-1 deletion, we found that TCF cKO CD8 T cells have increased expression of Eomes compared to WT CD8 T cells **(Fig. 3A)**. Other reports have claimed that T-bet may be activated or not affected by TCF-1 (14), but we found that loss of TCF-1 led to increased T-bet expression in CD8 T cells **(Fig. 3B)**. This suggests that TCF-1 normally suppresses expression of Eomes and T-bet in mature T cells. Next, we looked at T cell activation using CD44 and CD122Expression of CD122 was increased in TCF-1-deficient donor cells **(Fig. 3C)**. CD44 expression was polarized more potently among CD8 T cells from TCF cKO mice **(Fig. 3D-E)**. Some reports have suggested that $CD44^{hi}$ T cells do not cause GVHD or cause less severe GVHD (10, 32). Therefore, using CD62L and CD44, we identified four major memory subsets: central memory (44+ 62L+), effector memory (44+ 62L-), naive (44-), and activating/transitioning (44 mid) cells. TCF cKO mice had increased central memory CD8 T cells, and decreased transitioning/activating CD8 T cells **(Fig. 3E)**. Thus, loss of TCF-1 results in a more memory-skewed phenotype for CD8 T cells. Some reports have suggested that memory T cells delay induction of GVHD (10, 32), so this phenotypic change may be beneficial.

Changes to cell phenotype in a knock-out mouse may be cell-intrinsic (due directly to gene deficiency within the cell) or cell-extrinsic (due to changes in the microenvironment from gene deficiency). To determine whether the phenotypic effects we observed were cell-intrinsic or cell-extrinsic, we developed a chimeric mouse model. Briefly, we mixed bone marrow from WT and TCF cKO mice at a 1:4 (WT:TCF) ratio for a total of $50x10^6$ BM cells, then used this mixture to reconstitute lethally irradiated Thy1.1 mice. We used a 1:4 ratio to ensure survival of the KO cells (based on our initial observations that TCF cKO T cells do not proliferate well in

culture). At 9 weeks post-transplant, blood was taken to ensure reconstitution and survival of both donor types in each mouse. At 10 weeks, splenocytes were phenotyped by flow cytometry, with donor cells being identified by H2Kb, CD45.1 (WT), and CD45.2 (TCF cKO) markers **(Fig. 3F-I)**. TCF cKO donor CD8 T cells from the chimera still had increased expression of T-bet **(Fig. 3G)**, and expression of Eomes and CD122 were also increased to near-KO levels in WT donor cells **(Fig. 3F,H)**. This suggests that while phenotypic changes are primarily cell-intrinsic in the TCF cKO mice, some cell-extrinsic effects are also present. CD8 central memory cells were decreased in TCF cKO cells from the chimera (rather than being increased as in pre-transplant cells), suggesting that this effect is cell-extrinsic **(Fig. 3I)**. Chimeric TCF cKO donor cells also showed an increase in naive cells, which was unique to the chimera **(Fig. 3I)**. The decrease in transitioning cells was also preserved in chimeric TCF cKO cells, suggesting it is a cell-intrinsic effect **(Fig. 3I)**. Thus, the phenotypic changes induced in CD8 T cells by loss of TCF-1 are primarily cell-intrinsic, with some additional cell-extrinsic effects.

Loss of TCF-1 alters cytokine and cytotoxic mediator production by mature alloactivated CD8 T cells. One of the hallmarks of GVHD is the release of pro-inflammatory cytokines and cytotoxic mediators by alloactivated donor T cells, eventually leading to cytokine storm. These mediators also drive the GVL effect, which kills residual malignant cells. We examined whether loss of TCF-1 in donor CD8 T cells led to changes in cytokine or cytotoxic mediator production, thereby affecting GVHD damage. We allotransplanted lethally irradiated BALB/c mice as described above, with mice receiving $1.5X10^6$ WT or TCF cKO CD3 donor T cells, along with T cell-depleted BALB/c bone marrow. Recipients were sacrificed at day 7 post-transplant. Splenocytes were isolated and restimulated by 6 hours of culture with PBS (control) or anti-

CD3/anti-CD28 (stimulation), along with Golgiplug. Afterwards, the cultured cells were stained with antibodies against H2Kb, CD3, CD4, CD8, TNF-α, and IFN-γ. Our data showed that production of TNF-α by donor CD8 T cells trended toward decreasing when TCF-1 was lost **(Fig. 4A)**. In contrast, IFN-γ trended toward increasing upon loss of TCF-1 in CD8 T cells **(Fig. 4B)**. This suggests that TNF-α is more critical for GVHD-related damage by T cells than IFN-γ is.

We also obtained serum from cardiac blood of recipient mice at day 7 post-transplant, and tested it with a mouse Th cytokine ELISA panel (LEGENDplex kit from Biolegend). TNF-α in serum of mice given TCF cKO CD8 T cells was lower than in mice given WT CD8 T cells at day 7 **(Fig. 4C)**. Additionally, TNF-α levels in serum appeared to decrease over time past day 7 for both groups of mice, especially those given WT T cells **(Fig. 4C)**. When compared alone, serum from day 14 also showed a significant drop in TNF-α levels for TCF cKO-transplanted mice **(Fig. 4D)**. Interestingly, the same trend of decreasing levels in TCF cKO-transplanted mice was seen for IFN-γ in the serum **(Fig. 4E-F)**. This suggests that TCF cKO CD8 T cells may be capable of more IFN-γ production than WT cells when restimulated, but in reality, produce less IFN-γ than WT cells when allotransplanted. We also examined IL-2 levels, and found that they were increased in TCF cKO transplanted mice at day 7, supporting the early rise in proliferation, but drop below WT levels at day 14 and 21, supporting the hypothesized drop in proliferation as disease resolves **(Fig. 4G)**.

CD8 T cells primarily use cytotoxic molecules such as perforin and Granyzme B to mediate GVL effects (33). We looked at perforin and Granzyme B protein levels by performing a western blot on lysates from naive CD8 T cells or allotransplanted CD8 T cells from WT and TCF cKO mice. We found that naive TCF cKO CD8 T cells show a trend towards producing

more perforin and Granzyme B than WT CD8 T cells **(Fig. 4H-J)**. We also found that alloactivated TCF cKO CD8 T cells trend towards still producing more Granzyme B than WT CD8 T cells, with little to no difference in perforin expression compared to WT **(Fig. 4H,K-L)**. These results suggest that the GVL effect is maintained by TCF cKO T cells because they have more expression on a per-cell basis of cytotoxic mediators which are critical to this process.

TCF-1 controls chemokine and chemokine receptor expression of donor CD8 T cells during alloactivation. One of the major functions of alloactivated T cells is migration from spleen to GVHD target organs, including liver and small intestine. Given that GVHD severity is significantly reduced when donor T cells lack TCF-1, we examined whether these donor cells have defects in migration to target organs. To do this, we allotransplanted lethally irradiated BALB/c mice as described above, but with the donor cells being a 1:1 mixture of WT:TCF cKO (or WT:WT as control) CD3+ T cells. A total of $1X10^6$ T cells were injected, and prior to transplant the donor cells were checked to ensure a 1:1 ratio of donor types, as well as to ensure an approximately 1:1 distribution of CD4 and CD8 T cells **(Fig. 5A)**. WT Ly5.1 donors were identified with CD45.1, and TCF cKO or WT C57 donors were identified with CD45.2. At day 7, the spleen, lymph nodes, small intestine, and liver were removed from recipient mice and examined for expression of H2Kb, CD45.1, and CD45.2 to determine relative migration of donor T cells **(Fig. 5A)**.

For CD8 T cells, TCF cKO cells were present at slightly lower frequencies in guts, indicating a potential mild migration defect **(Fig. 5A)**, **(Supp. Fig. 2)**. However, this mild reduction in TCF cKO donor cells was also observed in the spleen, indicating that either a very mild migration defect, or more likely a mild proliferation defect, caused the decrease **(Fig. 5A)**,

(Supp. Fig. 2). Therefore, loss of TCF-1 likely does not significantly impact migration of allaoctivated CD8 T cells to target organs.

Expression of chemokines and chemokine receptors is a critical aspect of T cell migration to target organs. To determine whether expression of these molecules was affected by loss of TCF-1 in CD8 T cells, we FACS sorted pre- and post-transplanted donor CD8 T cells from WT or TCF cKO mice (spleen only for pre-transplant, spleen or liver for post-transplant). We then extracted RNA from the cells, converted it to cDNA, and performed qPCR using a 96-well mouse chemokine/chemokine receptor plate (Thermo Fisher). As expected, expression of these markers was generally upregulated in alloactivated cells. Expression of these markers was higher in TCF cKO CD8 T cells from pre-transplant spleen compared to WT pre-transplant spleen **(Fig. 5B)**, but these markers were downregulated in TCF cKO CD8 T cells from post-transplant liver and spleen compared to WT cells **(Fig. 5C-D)**. Therefore, TCF-1 controls expression of CD8 T cell chemokine/chemokine receptors, but loss of this factor has little to no impact on migration of these cells to target organs. Of note, a migration defect may become more apparent as the disease course continues, given that GVHD resolves over time in TCF cKO transplanted mice.

TCF-1 controls proliferation, apoptosis, and exhaustion of mature alloactivated CD8 T cells.

In order for GVHD to persist, donor T cells must proliferate in secondary lymphoid organs and target organs (34, 35). Naive and effector T cells drive GVHD, but they are short-lived and must be replaced to maintain an alloresponse (35, 36). Given that memory cells are increased and transitioning/activating cells are decreased among CD8 T cells when TCF-1 is lost, we hypothesized that proliferation, survival, or exhaustion of these cells may also be affected. To examine proliferation of these cells, BALB/c mice were allotransplanted as described above,

with mice receiving $1X10^6$ donor CD3 T cells (WT or TCF cKO) and $10X10^6$ BALB/c BM cells. Recipient mice were given 25mg/kg of EdU in PBS (i.p. injection) on day 5 and 6 to label proliferating cells. On day 7 post-transplant, we euthanized recipient mice and obtained lymphocytes from spleen and liver. These cells were stained with an EdU click chemistry kit (Invitrogen) to detect EdU-stained (proliferating) cells by flow cytometry. There was an increase in proliferation in the spleen and liver by CD8 TCF cKO T cells, which was significant in the liver **(Fig. 6A-B)**. Therefore, proliferation at day 7 is increased in TCF cKO CD8 T cells. We also used Ki67 staining in a similar but separate allo-HSCT experiment (without injecting EdU) to confirm these results, as Ki67 is a marker of T cell activation and proliferation. Indeed, Ki67 expression was increased or trending towards increased for TCF cKO CD8 T cells in the spleen and liver, respectively **(Fig. 6C-D)**. Therefore, proliferation in CD8 T cells early after alloactivation is increased by loss of TCF-1. However, given that symptoms of GVHD resolve after day 7 in TCF cKO-transplanted recipients **(Fig. 1A)**, we hypothesize that proliferation of donor cells decreases below WT levels after this point.

Impaired survival of donor T cells following allotransplant could also explain the reduction in disease. To test this, we performed a death assay by allotransplanting recipient mice as described with $10X10^6$ BALB/c BM cells and $1X10^6$ donor CD3 T cells (WT or TCF cKO). At day 7 post-transplant, recipient mice were euthanized, we obtained cells from spleen and liver, and stained them with antibodies against H2Kb, CD3, CD4, and CD8, as well as Annexin V-FITC, and LIVE/DEAD Near-IR. This allowed us to identify donor CD8 T cells, and further to separate three distinct populations - live cells, dead cells, and apoptotic cells **(Fig. 6E-F).** When we compared WT and TCF cKO donor cells in the spleen, we found that TCF cKO CD8 T cells were trending towards less frequently dead, and more frequently live or apoptotic, than WT

donor cells **(Fig. 6E)**. There appeared to be no difference in apoptosis or cell death in the liver **(Fig. 6F)**. This suggests that CD8 T cells lacking TCF-1 in the spleen may be more prone to apoptosis following allotransplant, suggesting a similar role for TCF-1 in survival of mature cells as for developing cells in the thymus (37, 38). In support of this, when we attempted to sort CD8 T cells from WT and TCF cKO-transplanted mice at day 7 post-transplant (in a separate experiment), there were significantly fewer CD8 donor T cells in the spleen from TCF cKO donors than from WT donors (by number of cells/10,000 total sorted cells) **(Supp. Fig. 3A)**. Donor cells also trended towards reduced for TCF cKO cells in the liver at day 7 **(Supp. Fig. 3B)**. In addition, we attempted to sort TCF cKO donor CD8 cells from recipient mice at day 14 post-transplant, and donor cells in the spleen and liver were trending towards reduced compared to WT and TCF cKO donor CD8 T cells from day 7 **(Supp. Fig. 3A-B)**. When we attempted to culture TCF cKO T cells using anti-CD3/anti-CD28 with or without IL-2, we found that they proliferate poorly in culture compared to WT T cells even when activated, making *in vitro* work very difficult (empirical observations). Therefore, it is likely that survival and/or proliferation are reduced after day 7 in TCF cKO CD8 T cells, giving rise to the progressive resolution in symptoms observed in TCF cKO-transplanted mice.

Finally, it is also possible that the donor T cells lacking TCF-1 become exhausted shortly after being transplanted. To determine whether this is occurring, we allotransplanted recipient mice as described with $10X10^6$ BALB/c BM cells and $1X10^6$ donor CD3 T cells (WT or TCF cKO). At day 7 post-transplant we stained cells from the spleen and liver for TOX, a marker of T cell exhaustion. We found that donor CD8 T cells from TCF cKO mice were significantly more exhausted in the spleen, and trending towards more exhausted in the liver, than WT donor cells **(Fig. 6G-H)**. Together, these data suggest that CD8 donor T cells from TCF cKO mice have

more frequent apoptosis, increased exhaustion, and a potential progressive defect in proliferation or survival over time compared to WT CD8 T cells. This provides a clinically optimal phenotype, because the donor cells eradicate residual malignant cells quickly after being transplanted, but then die off or become non-functional, removing the threat of host tissue damage. This observation helps to explain why GVHD score reduces rather than persisting over time for TCF cKO-transplanted mice **(Fig. 1A)**, as donor TCF cKO T cells may no longer be functional after day 7.

Loss of TCF-1 alters suppressive profile of T cells. To determine whether loss of TCF-1 also impacted the suppressive profile of donor T cells, $1X10^6$ WT or TCF cKO CD8 T cells were allotransplanted into recipient BALB/c mice with $10X10^6$ BALB/c BM cells as described. Lymphocytes were isolated from spleen and liver of the recipient mice at day 7, day 14, and day 21 post-transplant for phenotyping. We examined expression of PD-1, PD-L1, and CTLA-4 **(Supp. Fig. 4)**. TCF cKO CD8 T cells had lower expression of PD-1 in both spleen and liver at day 14 and 21 post-transplant, but not day 7 post-transplant **(Supp. Fig. 4-A-B)**. These data suggest that CD8 T cells from TCF cKO mice may be less susceptible to suppression by tumor cells (or other cells) expressing PD-L1 (39-41). Therefore, these T cells are more likely to be effective at killing target cells, because they are less capable of being turned off when a response is appropriate. However, this phenotypic change also increases the risk of autoreactive damage. Despite this, GVHD score and histology sections show reduced tissue damage for TCF cKO-transplanted mice **(Fig. 1A-E)**.

Expression of PD-L1 was increased in the spleen only for mice given TCF cKO CD8 T cells, at days 14 and 21 post-transplant **(Supp. Fig. 4C-D)**. The exact function of PD-L1

expressed on T cells is unknown, but it is thought to promote tumor tolerance by suppressing activation and promoting apoptosis of other T cells (42). Therefore, the higher expression of PD-L1 suggests that T cells that do not migrate to peripheral tissues by later time points after transplant are capable of suppressing other T cells around them. Thus, the loss of TCF-1 may induce a T cell phenotype which is both less susceptible to external suppression and more capable of suppressing other T cells. This may result in enhanced tumor killing with minimal damage to healthy bystander cells.

Expression of CTLA-4 was unaffected by loss of TCF-1 in donor CD8 T cells, both in liver and spleen **(Supp. Fig. 4E-F)**. CTLA-4 is responsible for turning off activation signaling resulting from TCR activation (43). Therefore, this data suggests that TCF cKO cells do not suffer from abnormal suppression or prolongation of TCR signaling due to improper regulation. These cells most likely are not always “on” or always “off” with regard to activation.

Reduced CXCR5 expression in CD8 T cells of TCF-1 deficient mice may contribute to reduced GVHD severity. CXCR5 is a major T cell chemokine receptor which contributes to T cell migration out of the spleen, although CXCR5 is traditionally described as a T follicular helper (Tfh) cell subset marker. In situations where antigen persists over a long period of time, such as during immunization or chronic viral infection, some CD8+ T cells also express CXCR5. These cells have been described as stem-like, and maintain the pool of exhausted CD8+ T cells during the immune response in these contexts (23). These cells are also responsible for proliferation and response to PD-1 blockade (44). In GVHD, alloantigens that are recognized by donor T cells come from the patient’s HLA molecules, so these antigens are chronically present. We hypothesized that persistence of GVHD damage over time results from the presence of CXCR5+

CD8+ T cells, which maintain the pool of cells capable of responding to alloantigen and causing damage. In this model, CXCR5+ CD8+ T cells in the spleen proliferate continuously, allowing waves of CD8 T cells to migrate to target organs, causing damage continuously.

To examine whether this hypothesis was correct, we looked at CXCR5 expression in naïve and alloactivated WT CD8+ T cells **(Fig. 7)**. In naïve WT T cells, CXCR5 expression among CD8+ T cells was low **(Fig. 7A)**. After alloactivation for 7, 14, or 21 days in allotransplanted mice, donor splenic WT CD8+ T cells expressed CXCR5 at a higher frequency than naïve cells**(Fig. 7A-D)**. Importantly, this CXCR5 expression remained higher than naïve levels at all timepoints after alloactivation, with a peak in expression around day 7 **(Fig. 7A-D)**. In addition, donor CD8+ T cells found in the liver also expressed CXCR5 at low levels, and this expression did not change over time post-alloactivation **(Fig. 7E-G)**. Together, these data support the hypothesis that in allotransplanted mice receiving WT donor T cells, CXCR5+ CD8+ T cells do exist. These cells persist over time, and may contribute both to ongoing damage, and to continual migration of donor cells into the liver and other target organs.

Previous reports suggest that TCF-1 is the single most critical transcription factor responsible for development of these Tfh-like CXCR5+ CD8+ T cells (45). Therefore, we examined whether CXCR5 expression is reduced when TCF-1 is lost in these cells. The frequency of CXCR5+ CD8+ T cells is not significantly lower in naive TCF cKO mice than in naive WT mice **(Fig. 7A)**. However, upon alloactivation, CD8+ T cells from TCF cKO donor mice had lower expression of CXCR5 in spleen at all time points, especially at day 14 and day 21 **(Fig. 7A-D)**. Although not significantly different from WT mice, the expression of CXCR5 among CD8+ donor T cells from the TCF cKO mice also trended towards decreasing over time in the liver **(Fig. 7E-G)**, suggesting that these cells do not persist or are not replaced by

subsequent waves of migrating cells when TCF-deficient donor cells are used for transplant. Thus, these data support the conclusion that TCF-1 is indeed important for development of CXCR5+ CD8+ T cells, but loss of TCF-1 only in T cells does not completely abrogate their development. Instead, frequencies of these cells are reduced in the TCF cKO donor cells during allotransplant, which we hypothesize may lead to impaired migration, and thus, reduced persistence and severity of GVHD-driven damage.

TCF-1 contributes to control of cell survival and immune signaling pathways in CD8 donor T cells. Given that the phenotype and functions of donor T cells, as well as disease outcomes, were significantly altered by loss of TCF-1 on donor cells, we sought to determine what specific gene changes occurred to support this. We allotransplanted recipient BALB/c mice with $10X10^6$ BALB/c BM and $1X10^6$ donor CD3 T cells as above, and FACS-sorted pre- and post-transplant WT or TCF cKO donor CD8 T cells, which were stored in Trizol . RNA sequencing was then performed (prep by SUNY Upstate Molecular Analysis Core, sequencing by University at Buffalo Genomics Core). Data were analyzed in Partek Flow **(Fig. 8)**. We found that WT and TCF cKO donor CD8 T cells cluster together both by strain and by timepoint (pre- and post-transplant) **(Fig. 8A)**. **(Supp. Fig. 5A-C)**. Numerous genes were affected by loss of TCF-1 in post-transplant donor cells, with cells in both spleen and liver affected **(Fig. 8B)**. Changes to Tbx21 (T-bet), as well as Cxcr4 and Ccr4 (chemokine receptors) were observed in pre-transplant CD8 donor T cells lacking TCF-1 **(Supp. Fig. 5D)**. As before, significant genes were determined by p-value ≤ 0.05 for pre-transplant cells. In post-transplant spleen, changes to IFNg (IFN-γ), Tbx21 (T-bet), Prf1 (perforin), and Il2rb (CD122) were observed for TCF cKO cD8 T cells **(Fig. 8C)**. In liver, TCF-1-deficient CD8 donor T cells showed changes to IFN-γ and Cxcr6

(chemokine receptor) **(Fig. 8D)**. These data support our earlier findings that expression of chemokines/chemokine receptors, as well as cytokines and cytotoxic mediators, are regulated by TCF-1 in mature alloactivated CD8 T cells.

Pathway enrichment analysis in pre-transplant CD8 donor cells showed that loss of TCF-1 affected T cell differentiation, cell adhesion, many signaling pathways (MAPK, NFκB, calcium, and others), and TCR signaling **(Supp. Fig. 5E)**. This analysis was determined using p-values rather than False Discovery Rate (FDR), as no significantly different features were detected with FDR ≤ 0.05. Following transplant, many pathways were affected by loss of TCF-1, in both spleen and liver-derived donor CD8 T cells. In both organs, loss of TCF-1 impacted cell cycle, necroptosis, cell senescence, and autophagy pathways **(Fig. 8E-F)**. This supports the idea that CD8 T cells are more prone to apoptosis or other forms of cell death when TCF-1 is lost, leading to donor cell loss after allotransplant. In the liver, NOD- and TCR-signaling were also affected, while in spleen, metabolism, DNA replication, T cell differentiation, NFκB signaling, and TNF signaling were impacted **(Fig. 8E-F)**.

Finally, we looked at expression levels of CXCR5 in D7 post-transplant donor CD8 T cells from spleen and liver, comparing WT and TCF cKO samples. We found that CXCR5 expression level was trending towards decreased in TCF cKO donor cells at D7 **(Fig. 8G)**, confirming the results that we obtained by flow cytometry **(Fig. 7)**. Although CXCR5 was not identified as a significantly changed gene (d7 spleen had p-value 0.041 but FDR 0.114, d7 liver had p-value 0.074 and FDR 0.179), the fold change for this gene was relatively large in spleen (8.392), which agrees with our flow cytometry data. Therefore, it is likely that loss of CXCR5 in CD8 T cells is an important factor in the reduced GVHD seen from TCF-deficient donor cells. Overall, these results show that TCF-1 controls a wide range of immune-related gene programs in mature and

allaoctivated CD8 T cells. Loss of TCF-1 in donor cells leads to a favorable phenotype following allotransplant, primarily through altered gene expression that leads to altered T cell function.

Discussion

In this manuscript, as well as in our companion manuscript, we identified T Cell Factor-1 (TCF-1) as a critical regulatory transcription factor for alloactivated mature T cells. TCF-1 is known to be important for T cell development, as well as activation in some contexts (46) (47). However, it was previously unknown whether TCF-1 played a role in regulating mature and alloactivated T cells. Here, we show that loss of TCF-1 separates GVHD from GVL driven by CD8 T cells in a clinically optimal fashion. While TCF-1 in donor T cells is dispensable for GVL effects, it is essential for host tissue damage during GVHD. Importantly, we show here and in our companion manuscript that the role of TCF-1 in regulating these T cells in unique in CD8 versus CD4 T cells.

Using our unique mouse model with T cell-specific deletion of TCF-1 rather than global deficiency, we were able to study mature CD8 T cells in an allo-HSCT model. This murine model allows us to study T cell function, clinical outcomes, and gene expression all in one model. Here, we showed that TCF-1-deficient donor CD8 T cells produce less severe and persistent GVHD than WT CD8 T cells. Additionally, tissue damage in liver, skin, and small intestine (all target organs) was reduced by loss of TCF-1 in donor CD8 T cells. This shows that TCF-1 in donor T cells is required for GVHD damage and persistence over time. Importantly, GVL effects were not disrupted by loss of TCF-1, suggesting that TCF-1 is dispensable for GVL effects. This was mostly likely due to an increase in perforin and granzyme B pre-transplant, as well as increased granzyme B post-transplant for TCF-1-deficient CD8 T cells. Increased expression of Eomes and T-bet may also have contributed to GVL effects (10, 16) (48). This suggests that despite other functional changes which disrupt GVHD damage, the increase in cytotoxic mediators helps maintain GVL effects driven by TCF cKO CD8 T cells.

We also examined the major alloactivated T cell functions – migration, proliferation, and cytokine production – to better understand how TCF-1 regulates mature T cells to provide an optimal disease phenotype. We showed that loss of TCF-1 in donor CD8 T cells leads to reduced production of TNF-α (yet increased IFN-γ production), increased predisposition to apoptosis, increased exhaustion, and possibly reduced proliferation of alloactivated donor T cells. The reduced survival of and production of TNF-α by donor CD8 T cells leads to the reduction in GVHD severity. However, expression of perforin and Granyzme B were increased, allowing these cells to maintain GVL effects despite their functional handicaps. In addition, although no major migration defect was detected, loss of TCF-1 altered expression of chemokines and chemokine receptors on donor CD8 T cells, both pre- and post-transplant. This phenotype caused by loss of TCF-1 is clinically optimal, because it allows for clearance of residual malignant cells while limiting the risk of life-threatening GVHD damage.

When we attempted to FACS-sort donor T cells from recipients at day 7, we found that donor cell numbers for the TCF cKO-transplanted mice were significantly reduced in spleen and trending towards reduced in liver. T cell survival must occur for persistence of GVHD responses(36). These data support the idea that TCF-1-deficient donor cells are either dying or not proliferating following transplant, which correlates with the observed increase in apoptotic cells, as well as the reduction in disease severity beyond day 7 post-transplant. This observation, coupled with the increase in exhaustion of TCF cKO donor CD8 T cells, suggests that donor cells lacking TCF-1 are highly activated and cytotoxic to malignant cells early on following transplant, but quickly die off or become exhausted, limiting GVHD progression. This also makes sense given the observation that proliferation is higher in TCF cKO cells at day 7, because we expect that these cells function normally or even better than WT cells, but then quickly lose

functionality and die off. Again, this is critical as loss of TCF-1 allows clearance of tumor cells through GVL effects, but after this point the donor cells no longer cause GVHD damage, resolving disease quickly and with less tissue damage.

When we phenotyped TCF cKO and WT CD8 T cells prior to transplant, we found an expansion of activated cells (CD122+, CD44+), as well as an increase in Eomes and T-bet expression. Eomes and T-bet are both linked to expression of cytotoxic mediators, such as perforin (Eomes) and IFN-γ (T-bet) (49, 50). In addition, we found that CD8 central memory T cells were expanded in TCF cKO mice. While effector and naive cells are known to cause severe GVHD, memory cells are often associated with less severe disease (10, 32), suggesting that this phenotypic change in TCF cKO cells may be beneficial for reducing disease severity. These phenotypic effects were primarily cell-intrinsic, and driven by loss of TCF-1. We also found that the suppressive profile of CD8 T cells is altered by loss of TCF-1. PD-1 expression was decreased and PD-L1 expression was increased on TCF cKO CD8 donor T cells late after transplant (day 14 and 21). This suggests that the donor cells may be less susceptible to suppression by PD-L1+ cells (such as tumor cells), and may be more capable of suppressing other nearby cells (26, 51). This could allow donor T cells lacking TCF-1 to attack tumor cells but also suppress nearby alloactivated donor cells to limit disease.

Recent work has identified a CXCR5+ subset of CD8 T cells that arises following chronic antigen stimulation. These cells are stem-like, and are thought to maintain the pool of responding CD8 T cells during chronic immune responses (22, 23). Given that alloantigen is constantly presented during GVHD, we sought to determine whether this cell subset also exists in GVHD, and whether it may contribute to disease severity. Indeed, we found that CXCR5+ CD8+ donor-derived T cells are found in mice allotransplanted with WT donor T cells. These

mice develop severe GVHD and have poor survival. Interestingly, these cells appear to peak around day 7, which is typically the peak of disease severity by clinical scoring. We also found that the frequency of these CXCR5+ CD8+ donor T cells is reduced in mice allotransplanted with TCF cKO donor cells. TCF-1 is thought to be a critical factor for production of these cells (52) yet modulation of TCF-1 in CD8 T cells only reduces the frequency of these cells. Importantly, this reduction in CXCR5+ CD8+ T cells correlated with the pattern of reduced disease severity and persistence in TCF cKO-transplanted mice. RNAseq results from D7 post-transplant cells in spleen and liver show the same trend, with expression level of CXCR5 trending towards decreased in TCF cKO donor CD8 T cells. This suggests that CXCR5+ CD8+ T cells may be responsible for driving chronic responses to alloantigen during GVHD, and that depletion of this subset may prevent or reduce GVHD severity and persistence. Critically, GVL effects were maintained despite reduction in the frequency of these cells from TCF cKO donors, suggesting that CXCR5+ CD8+ T cells may be important for GVHD, but not GVL effects. Further modulation or depletion of this cell subset could therefore potentially separate GVHD from GVL effects.

Finally, to identify the changes to the genetic program of donor T cells that occurred in the absence of TCF-1, we performed RNA sequencing on pre- and post-transplant donor T cells. We found that CD8 donor T cells clustered together both by strain and by time (pre- and post-transplant), and that many genes were altered by TCF-1 deficiency. When comparing pre-transplant donor cells, no genes came up as significantly different when using FDR ≤ 0.05, most likely meaning that donor cells from WT and TCF cKO mice are similar pre-transplant. Therefore, p-value ≤ 0.05 was used to define significant genes for pathway analysis (for pre-transplant only). This also suggests that the changes to Eomes and T-bet expression seen in

phenotyping were due to post-transcriptional changes. In pre-transplant cells, TCF-1 deficiency led to changes in cell adhesion, TCR and other signaling pathways, and T cell differentiation, among others. Of note, post-transplant donor cells from both spleen and liver showed changes to necroptosis, cell cycle, autophagy, and cell senescence pathways. This strongly supports our *ex vivo* evidence that TCF cKO CD8 donor T cells are more prone to apoptosis, and therefore most likely die off following allotransplant, allowing disease to resolve. In addition, multiple immune signaling pathways such as NOD, NFκB, and TNF signaling were affected by loss of TCF-1. Therefore, TCF-1 controls these immune-related genetic programs in mature and allaoctivated CD8 T cells.

In our companion manuscript, we also address the role of TCF-1 in regulating alloactivated CD4 T cells. From this work, we found that regulation of CD4 versus CD8 T cells by TCF-1 is different, most likely due to the ability of TCF-1 to maintain lineage identity and alter gene expression in these subsets. Overall, our data show that TCF-1 plays a direct role in regulating mature CD4 and CD8 T cells during alloactivation. Loss of TCF-1 in CD8 T cells (as well as CD4 T cells) leads to reduced severity and persistence of GVHD, but maintains CD8 T cell-driven GVL effects. This may be due at least in part to reduction of CXCR5+ CD8+ donor-derived T cells, which correlate temporally with peak disease severity. Therefore, modulation of TCF-1, and possibly of CXCR5+ CD8 T cells, may separate GVHD from GVL to provide clinical benefit for allo-HSCT patients, or in treatment of other T cell-mediated diseases.

Materials and Methods

Mouse Models. For transplant, the following female donor mice were used: B6-Ly5.1 (CD45.1+, "WT" or B6.SJL-Ptprca Pepcb/BoyCrl, 494 from Charles River), C57Bl/6J (CD45.2+, "WT", 000664 from Jackson Laboratories), Tcf7 flox x CD4cre (referred to here as "TCF cKO" (17) , obtained from Dr. Jyoti Misra Sen at NIH by permission of Dr. Howard Xue, and bred in-house), or CD4cre (022071 from Jackson Laboratories, bred in-house). These donor mice were age-matched to each other and to recipients as closely as possible. BALB/c female mice (CR:028 from Charles River, age 8 weeks or older) were used as recipient mice for transplant experiments, and Thy1.1 mice (B6.PL-Thy1a/CyJ, 000406 from Jackson Labs) were used as recipient mice for chimera experiments.

Allotransplant and Tumor Models. BALB/c recipient mice were irradiated with two doses of 400 cGy of x-rays (total dose 800 cGy), and rested for at least 12 hours between doses. Mice were also rested for 4 hours prior to transplantation. T cells (total CD3+ or CD8+) were separated from WT, CD4cre, or TCF cKO spleens using CD90.2 or CD8 microbeads and LS columns (Miltenyi, CD8: 130-117-044, CD90.2: 130-121-278, LS: 130-042-401). $1X10^6$ donor cells were injected IV into the tail vein in PBS, along with $10X10^6$ BALB/c bone marrow cells. Bone marrow was T-cell depleted with CD90.2 MACS beads (130-121-278 from Miltenyi) and LD columns (130-042-901 from Miltenyi). For short-term experiments, at day 7 post-transplant, recipient mice were euthanized and serum, spleen, lymph nodes, small intestine, or liver were collected, depending on the experiment. For migration assay, a 1:1 ratio of WT (CD45.1):WT(CD45.2) or WT (CD45.1):TCF cKO (CD45.2) donor cells was used to make up the $1X10^6$ T cells. For GVHD and GVL experiments, recipient mice were also given $2X10^6$ B-

cell acute lymphoblastic leukemia (B-ALL) tumor cells expressing luciferase (10, 27). Recipient mice were weighed, given a clinical score, and imaged using the IVIS 200 imaging system three times per week until day 60 or longer. Clinical scores were composed of scores for skin integrity, fur texture, posture, activity, diarrhea, and weight loss. Imaging was done by injecting recipients i.p. with D-luciferin to detect tumor cell bioluminescence. To produce mixed bone marrow chimeras, Thy1.1 mice were lethally irradiated and reconstituted with a 1:4 (WT:TCF cKO) mixture of bone marrow cells (total $50x10^6$ cells), then rested for 9 weeks. At 9 weeks, tail vein blood was collected and checked by flow cytometry for CD45.1 and CD45.2 to ensure reconstitution with both donor cell types. At 10 weeks, mice were used for phenotyping experiments.

Flow Cytometry, Sorting, and Phenotyping. Splenocytes (or cells from other organs) were obtained from WT or TCF cKO mice or recipient allotransplanted mice. Lymphocytes were obtained and lysed with RBC Lysis Buffer (00-4333-57 from eBioscience) to remove red blood cells if needed. Cells were then stained with extracellular markers for 30 min on ice in MACS buffer (1X PBS with EDTA and 4g/L BSA). If intracellular markers were used, the cells were then fixed and permeabilized using the Fix/Perm Concentrate and Fixation Diluent from FOXP3 Transcription Factor Staining Buffer Set (eBioscience cat. No. 00-5523-00). The cells were then run on a BD LSR Fortessa cytometer and data was analyzed using FlowJo software v9 (Treestar). All antibodies were used at a 1:100 dilution. For FACS sorting, the same methods was applied, and cells were run on a BD FACS Aria IIIu with cold-sorting blocks. Cells were sorted into sorting media (50% FBS in RPMI) or Trizol, depending on the experiment. Depending on the experiment, antibodies used were: anti-CD4 (FITC, PE, BV785, BV21), anti-

CD8 (FITC, PE, APC, PerCP, Pacific Blue, PE/Cy7), anti-CD3 (BV605 or APC/Cy7), anti-H2Kb-Pacific Blue, anti-H2Kd-PE/Cy7, anti-CD122 (FITC or APC), anti-CD44 (APC or Pacific Blue), anti-CD62L (APC/Cy7), anti-TNF-α-FITC, anti-IFN-γ-APC, anti-Eomes (AF488 or PE/Cy7), anti-T-bet-BV421, anti-CD45.2-PE/Dazzle594, anti-CD45.1-APC, anti-Ki67 (PE or BV421), anti-PD-1-BV785, anti-CTLA-4-PE, and anti-PD-L1 (PE or PE/Dazzle594), anti-Annexin V-FITC, LIVE/DEAD Near IR, anti-EdU-AF647 (click chemistry kit), anti-TOX-APC, and anti-CXCR5-APC.

Histology. Recipient mice were allotransplanted as described, and organs were removed for histology at day 7, day 14, and day 21 post-transplant. Spleen, liver, small intestine, and skin (from ear and back) were fixed, sectioned, and stained with H&E at Cornell University (https://www.vet.cornell.edu/animal-health-diagnostic-center/laboratories/anatomic-pathology/services). A pathologist (A.M.) who was blinded to slide identity and study conditions then graded the sections for GVHD damage on a scale of 0-4. Criteria were: for skin - basal cell vacuolation up to frank epidermal denudation, for small intestine - single cell necrosis up to diffuse mucosal denudation, and for liver - percent of bile duct showing epithelial damage (I ≤25%, II 25-49%, III 50-74%, IV 75-100%).(53)(54).

Isolation of lymphocytes from liver, small intestine, or lymph nodes. Livers were perfused with 5-10mL of ice cold PBS to remove RBCs, then smashed through a 70uM filter with PBS. Cells were centrifuged to remove debris, and then spun for 22 minute spin in 40% Percoll in RPMI/PBS (22 degrees C, 2200rpm, no brake, no acceleration) to isolate lymphocytes. RBC Lysis Buffer was then used to remove any remaining RBCs, and cells were put into MACS

buffer (BSA in PBS). To obtain lymphocytes from gut, small intestine was removed to ice cold MACS buffer, cut open, and washed with MACS. Strip buffer (1XPBS, FBS, EDTA 0.5M, and DTT 1M) was used to remove epithelium (shaking for 30 min at 37 C), followed by mincing and incubation with digestion buffer (collagenase, DNAse, and RPMI) for 30 min at 37 C (while shaking). The gut pieces were vortexed and mashed through a 70uM filter with the liquid to obtain a cell suspension. Percoll was used as for liver to isolate lymphocytes from this suspension, but RBC lysis was not done. For lymph nodes, the inguinal, brachial, and axillary lymph nodes were taken from recipients and ground between glass slides. Cells were washed into a tube with MACS and spun to remove debris.

Cytokine Restimulation. Recipient BALB/c mice were allotransplanted with $1.5X10^6$ CD3 donor T cells and $10X10^6$ BALB/c BM, and euthanized at day 7. Splenocytes were taken and cultured for 6 hours with GolgiPlug (1:1000) and PBS (control) or anti-CD3 (1ug/mL)/anti-CD28 (2ug/mL) (TCR stimulation) at 37 C and 7% CO2. After 6 hours of culture, the cells were stained for CD3, CD4, CD8, H2Kb, TNF-α, and IFN-γ using the BD Cytokine Staining kit (BD Biosciences, 555028), and run on a flow cytometer.

LegendPLEX Serum ELISA Assay. Serum from cardiac blood was collected from recipient mice in the cytokine restimulation experiment. Serum was analyzed using the Biolegend LEGENDPlex Assay Mouse Th Cytokine Panel kit (741043). This kit quantifies serum concentrations of: IL-2 (T cell proliferation), IFN-y and TNF-a (Th1 cells, inflammatory), IL-4, IL-5, and IL-13 (Th2 cells), IL-10 (Treg cells, suppressive), IL-17A/F (Th17 cells), IL-21 (Tfh

cells), IL-22 (Th22 cells), IL-6 (acute/chronic inflammation/T cell survival factor), and IL-9 (Th2, Th17, iTreg, Th9 – skin/allergic/intestinal inflammation).

Western blot. Splenocytes from WT or TCF cKO donor mice, or from WT- or TCF cKO-transplanted recipient mice as described ($1X10^6$ CD8 donor T cells and $10X10^6$ BALB/c BM), were collected. CD8+ T cells were separated using CD8 MACS beads. These cells were counted and lysed with RIPA Buffer (89900 from Thermo Fisher) plus protease inhibitors (11697498001 from Millipore Sigma) to obtain lysates. The lysates were run on a Western blot and probed for perforin, Granzyme B, and actin.

Migration Assay. Recipient BALB/c mice were allotransplanted as before with $10X10^6$ BALB/c BM and $1X10^6$ donor CD3 T cells. However, the $1X10^6$ donor T cells were a 1:1 mixture of WT CD45.1+ CD3 T cells with either WT CD45.2+ cells or TCF cKO CD45.2+ cells. Prior to transplant, the donor cells were checked to ensure a 1:1 of CD4/CD8 T cells and of donor strain (WT:WT or WT:TCF cKO). 7 days post-transplant, recipients were euthanized and the spleen, lymph nodes, liver, and small intestine were removed. Lymphocytes were obtained from the organs as described, and stained for CD3, CD4, CD8, H2Kb, H2Kd, CD45.1, and CD45.2. The ratio of CD45.1 to CD45.2 cells was determined from flow cytometry data (i.e. WT to WT or WT to TCF cKO).

qPCR Analysis. To perform qPCR, BALB/c mice were allotransplanted as described ($1X10^6$ CD3 donor T cells and $10X10^6$ BALB/c BM). Pre-transplant donor cells and post-transplant (day 7) spleen and liver cells from recipients were FACS-sorted to obtain CD8+ donor cells. The cells

were sorted into Trizol, RNA was extracted using chloroform (https://www.nationwidechildrens.org/ Document/Get/93327), and eluted using the Qiagen RNEasy Minikit (74104 from Qiagen). Concentration was checked with a spectrophotometer, then RNA was converted to cDNA with an Invitrogen Super Script IV First Strand Synthesis System kit (18091050 from Invitrogen). Final cDNA concentration was checked with a spectrophotometer, then cDNA was mixed with Taqman Fast Advanced Master Mix (4444557 from Invitrogen) at a 10ng/uL cDNA concentration. This master mix was added to premade 96 well TaqMan Array plates with chemokine/chemokine receptor primers (Thermo Fisher, Mouse Chemokines & Receptors Array plate, 4391524). qPCR was performed in a Quant Studio 3 thermocycler, and data were analyzed using the Design and Analysis software v2.4 (provided by Thermo Fisher). Five separate recipient mice were sorted and cells were combined to make one sample for qPCR testing per condition/organ.

Proliferation Assay. Recipient BALB/c mice were allotransplanted as before ($1X10^6$ CD3 donor T cells and $10X10^6$ BALB/c BM). On day 5 and 6 post-transplant, recipient mice were injected i.p. with 25mg/kg of EdU in PBS. At day 7, recipient mice were euthanized and spleen and liver were processed to obtain lymphocytes. An EdU click chemistry kit (C10424 from Invitrogen) was used along with antibodies for CD3, CD4, CD8, and H2Kb to detect proliferating donor cells. *In vitro* culture attempts mentioned as empirical observations were done at 37 C, 7% CO2, with anti-CD3 (1ug/mL), anti-CD28 (2ug/mL), and in some cases, IL-2 (1000IU/mL).

Death Assay. To assess apoptosis and death in donor cells, recipient mice were allotransplanted as above ($1X10^6$ CD3 donor T cells and $10X10^6$ BALB/c BM). At 7 days post-transplant,

recipient mice were euthanized and spleen and liver were taken. Lymphocytes were obtained as described and stained with antibodies for CD3, CD4, CD8, and H2Kb to identify donor cells. The cells were also stained with Annexin V-FITC (V13242 from Invitrogen) and LIVE/DEAD Near IR (L34976 from Invitrogen). Annexin V and NIR were used to identify dead (Ann.V+NIR+), live (Ann.V-NIR-), and apoptotic (Ann.V+NIR-) cells.

Exhaustion/Activation Assay. To assess exhaustion and activation in donor cells, recipient mice were allotransplanted as before ($1X10^6$ CD3 donor T cells and $10x10^6$ BALB/c BM) and euthanized at day 7. Lymphocytes were obtained from spleen and liver, and stained for CD3, CD4, CD8, H2Kb, TOX, and Ki67.

Time course Assay. Recipient mice were allotransplanted as before ($1X10^6$ CD8 donor T cells and $10X10^6$ BALB/c BM), and euthanized at day 7, day 14, or day 21 in groups. Spleen and liver were taken from each mouse, and lymphocytes were isolated. The cells were stained for CXCR5, PD-1, PD-L1, CTLA-4, CD3, CD4, CD8, and H2Kb.

DNA Extraction and PCR. Donor mice were genotyped using PCR on DNA extracted from ear punches. At 4 weeks of age mice were ear punched, and DNA was extracted using the Accustart II Mouse Genotyping kit (95135-500 from Quanta Biosciences). Standard PCR reaction conditions and primer sequences from Jackson Laboratories were used for Eomes, T-bet, and CD4cre. For Tcf7, primer sequences and reaction conditions were obtained from Dr. Jyoti Misra Sen of NIH.

RNA Sequencing. Recipient mice were allotransplanted as before ($1X10^6$ CD3 donor T cells and $10X10^6$ BALB/c BM), except that donor CD8 T cells were also FACS-sorted prior to transplant. A sample of sorted donor cells was saved for RNA sequencing. At day 7 post-transplant, donor CD8 T cells were FACS-sorted back from recipient spleen and liver, and for TCF cKO-transplanted mice, cells were also collected at day 14. The cells were all sorted into Trizol, then RNA was extracted and prepped by the Molecular Analysis Core (SUNY Upstate, https://www.upstate.edu/research/facilities/molecular-analysis.php). Paired end sequencing was done with an Illumina NovaSeq 6000 system at the University at Buffalo Genomics Core (http://ubnextgencore.buffalo.edu). Data were provided and analyzed in Partek Flow. Data will be deposited (https://www.ncbi.nlm.nih.gov/geo/).

Statistical Analysis. Unless otherwise noted in the figure legends, all numerical data are presented as means and standard deviations with or without individuals points. Analysis was done in GraphPad Prism v7 or v9. Most data were analyzed with Student's t-test, one-way ANOVA, or two-way ANOVA, with Tukey's multiple comparisons test for ANOVA methods, depending on the number of groups. Chi-square analyses were done for GVHD histology grades. Kaplan-Meier survival analyses were done for survival experiments. All tests were two-sided, and p-values less than or equal to (≤) 0.05 were considered significant. Transplant experiments used 3-5 mice per group, with at least two repeats. *Ex vivo* experiments were done two to three times unless otherwise noted with at least three replicates per condition each time. RNAseq was done once with three replicates per group and condition. qPCR was done once with one sample per condition, and 5 mice combined to make the one sample. Sorting was done once for each of these two experiments, and data were recorded from one experiment for Supp. Fig. 3. The time

course assay was done once with 4-6 samples per group. Western blots were done twice for pre-transplant and once for post-transplant, one experiment each is shown.

Study Approval. All animal studies were reviewed and approved by the IACUC at SUNY Upstate Medical University. All procedures and experiments were performed according to these approved protocols.

Author Contributions

RH designed and conducted experiments, analyzed data, and wrote the manuscript. MK assisted with scientific/technical research design. MK and JMS edited the manuscript. MK and MM assisted with data collection. AM performed histology analyses. QY provided technical and scientific advice and assisted with data analysis. IF produced gene expression heatmaps for RNAseq data.

Acknowledgments

We thank all members of the Karimi lab for helpful discussions. This research was funded in part by a grant from the National Blood Foundation Scholar Award to MK, the National Institutes of Health (NIH LRP #L6 MD0010106 and K22 (AI130182) to MK), and an Upstate Medical University Cancer Center grant (1146249-1-75632) to MK. JMS was supported by the Intramural Research Program of the National Institute of Aging. We thank Dr. Howard Xue for permission to use TCF cKO mice. TCF cKO mice were provided by Dr. Jyoti Misra Sen from NIH. Flow cytometers and sorters were provided and maintained by Lisa Phelps of the SUNY Upstate Flow Core. RNA extraction and prep was done by Karen Gentile of the SUNY Upstate Molecular Analysis core, and RNA sequencing was done by the University at Buffalo Genomics Core.

References

1. Breems DA, and Lowenberg B. Autologous stem cell transplantation in the treatment of adults with acute myeloid leukaemia. *Br J Haematol.* 2005;130(6):825-33.
2. Blazar BR, Murphy WJ, and Abedi M. Advances in graft-versus-host disease biology and therapy. *Nat Rev Immunol.* 2012;12(6):443-58.
3. Ferrara JL, Levine JE, Reddy P, and Holler E. Graft-versus-host disease. *Lancet.* 2009;373(9674):1550-61.
4. Ferrara JL. Blood and Marrow Transplant Clinical Trials Network: Progress since the State of the Science Symposium 2007. *Biology of blood and marrow transplantation : journal of the American Society for Blood and Marrow Transplantation.* 2014;20(2):149-53.
5. Dickinson AM, Norden J, Li S, Hromadnikova I, Schmid C, Schmetzer H, et al. Graft-versus-Leukemia Effect Following Hematopoietic Stem Cell Transplantation for Leukemia. *Front Immunol.* 2017;8:496.
6. Murray J, Stringer J, and Hutt D. In: Kenyon M, and Babic A eds. *The European Blood and Marrow Transplantation Textbook for Nurses: Under the Auspices of EBMT*. Cham (CH); 2018:221-51.
7. Bell GM, Anderson AE, Diboll J, Reece R, Eltherington O, Harry RA, et al. Autologous tolerogenic dendritic cells for rheumatoid and inflammatory arthritis. *Ann Rheum Dis.* 2017;76(1):227-34.
8. Gam R, Shah P, Crossland RE, Norden J, Dickinson AM, and Dressel R. Genetic Association of Hematopoietic Stem Cell Transplantation Outcome beyond Histocompatibility Genes. *Front Immunol.* 2017;8:380.
9. Ghimire S, Weber D, Mavin E, Wang XN, Dickinson AM, and Holler E. Pathophysiology of GvHD and Other HSCT-Related Major Complications. *Front Immunol.* 2017;8:79.
10. Mammadli M, Huang W, Harris R, Sultana A, Cheng Y, Tong W, et al. Targeting Interleukin-2-Inducible T-Cell Kinase (ITK) Differentiates GVL and GVHD in Allo-HSCT. *Front Immunol.* 2020;11:593863.
11. Bleakley M, Heimfeld S, Jones LA, Turtle C, Krause D, Riddell SR, et al. Engineering human peripheral blood stem cell grafts that are depleted of naive T cells and retain functional pathogen-specific memory T cells. *Biology of blood and marrow transplantation : journal of the American Society for Blood and Marrow Transplantation.* 2014;20(5):705-16.
12. Sharma A, Berga-Bolanos R, and Sen JM. T cell factor-1 controls the lifetime of CD4+ CD8+ thymocytes in vivo and distal T cell receptor alpha-chain rearrangement required for NKT cell development. *PLoS One.* 2014;9(12):e115803.
13. Germar K, Dose M, Konstantinou T, Zhang J, Wang H, Lobry C, et al. T-cell factor 1 is a gatekeeper for T-cell specification in response to Notch signaling. *Proc Natl Acad Sci U S A.* 2011;108(50):20060-5.
14. Ma J, Wang R, Fang X, and Sun Z. beta-catenin/TCF-1 pathway in T cell development and

918 differentiation. *J Neuroimmune Pharmacol.* 2012;7(4):750-62.
919 15. Paley MA, and Wherry EJ. TCF-1 flips the switch on Eomes. *Immunity.* 2010;33(2):145-7.
920 16. Fu J, Wang D, Yu Y, Heinrichs J, Wu Y, Schutt S, et al. T-bet is critical for the development
921 of acute graft-versus-host disease through controlling T cell differentiation and function.
922 *J Immunol.* 2015;194(1):388-97.
923 17. Steinke FC, Yu S, Zhou X, He B, Yang W, Zhou B, et al. TCF-1 and LEF-1 act upstream of
924 Th-POK to promote the CD4(+) T cell fate and interact with Runx3 to silence Cd4 in
925 CD8(+) T cells. *Nat Immunol.* 2014;15(7):646-56.
926 18. Bouazzaoui A, Spacenko E, Mueller G, Miklos S, Huber E, Holler E, et al. Chemokine and
927 chemokine receptor expression analysis in target organs of acute graft-versus-host
928 disease. *Genes Immun.* 2009;10(8):687-701.
929 19. Henden AS, and Hill GR. Cytokines in Graft-versus-Host Disease. *J Immunol.*
930 2015;194(10):4604-12.
931 20. Hill GR, and Koyama M. Cytokines and costimulation in acute graft-versus-host disease.
932 *Blood.* 2020;136(4):418-28.
933 21. Zhang J, Chen HM, Ma G, Zhou Z, Raulet D, Rivera AL, et al. The mechanistic study
934 behind suppression of GVHD while retaining GVL activities by myeloid-derived
935 suppressor cells. *Leukemia.* 2019;33(8):2078-89.
936 22. Kircher B, Schumacher P, and Nachbaur D. Granzymes A and B serum levels in allo-SCT.
937 *Bone Marrow Transplant.* 2009;43(10):787-91.
938 23. Valentine KM, and Hoyer KK. CXCR5+ CD8 T Cells: Protective or Pathogenic? *Front*
939 *Immunol.* 2019;10:1322.
940 24. Im SJ, Konieczny BT, Hudson WH, Masopust D, and Ahmed R. PD-1+ stemlike CD8 T cells
941 are resident in lymphoid tissues during persistent LCMV infection. *Proc Natl Acad Sci U S*
942 *A.* 2020;117(8):4292-9.
943 25. Shen Y, Qu QX, Jin MN, and Chen C. Investigating the role of circulating CXCR5-
944 expressing CD8+ T-cells as a biomarker for bacterial infection in subjects with
945 pneumonia. *Respir Res.* 2019;20(1):54.
946 26. Flowers ME, and Martin PJ. How we treat chronic graft-versus-host disease. *Blood.*
947 2015;125(4):606-15.
948 27. Cheng Y, Chikwava K, Wu C, Zhang H, Bhagat A, Pei D, et al. LNK/SH2B3 regulates IL-7
949 receptor signaling in normal and malignant B-progenitors. *J Clin Invest.*
950 2016;126(4):1267-81.
951 28. Cooke KR, Kobzik L, Martin TR, Brewer J, Delmonte J, Jr., Crawford JM, et al. An
952 experimental model of idiopathic pneumonia syndrome after bone marrow
953 transplantation: I. The roles of minor H antigens and endotoxin. *Blood.* 1996;88(8):3230-
954 9.
955 29. Pidala J, Kim J, Anasetti C, Nishihori T, Betts B, Field T, et al. The global severity of
956 chronic graft-versus-host disease, determined by National Institutes of Health consensus
957 criteria, is associated with overall survival and non-relapse mortality. *Haematologica.*
958 2011;96(11):1678-84.
959 30. https://www.uptodate.com/contents/clinical-manifestations-diagnosis-and-grading-of-
960 acute-graft-versus-host-disease
961 31. Sun R, Wu Y, Zhou H, Wu Y, Yang Z, Gu Y, et al. Eomes Impedes Durable Response to

962 Tumor Immunotherapy by Inhibiting Stemness, Tissue Residency, and Promoting the
963 Dysfunctional State of Intratumoral CD8(+) T Cells. *Front Cell Dev Biol.* 2021;9:640224.
964 32. Dutt S, Baker J, Kohrt HE, Kambham N, Sanyal M, Negrin RS, et al. CD8+CD44(hi) but not
965 CD4+CD44(hi) memory T cells mediate potent graft antilymphoma activity without
966 GVHD. *Blood.* 2011;117(11):3230-9.
967 33. Du W, and Cao X. Cytotoxic Pathways in Allogeneic Hematopoietic Cell Transplantation.
968 *Front Immunol.* 2018;9:2979.
969 34. Beilhack A, Schulz S, Baker J, Beilhack GF, Wieland CB, Herman EI, et al. In vivo analyses
970 of early events in acute graft-versus-host disease reveal sequential infiltration of T-cell
971 subsets. *Blood.* 2005;106(3):1113-22.
972 35. Paczesny S, Hanauer D, Sun Y, and Reddy P. New perspectives on the biology of acute
973 GVHD. *Bone Marrow Transplant.* 2010;45(1):1-11.
974 36. Chakraverty R, and Sykes M. The role of antigen-presenting cells in triggering graft-
975 versus-host disease and graft-versus-leukemia. *Blood.* 2007;110(1):9-17.
976 37. Ioannidis V, Beermann F, Clevers H, and Held W. The beta-catenin--TCF-1 pathway
977 ensures CD4(+)CD8(+) thymocyte survival. *Nat Immunol.* 2001;2(8):691-7.
978 38. Xu Z, Xing S, Shan Q, Gullicksrud JA, Bair TB, Du Y, et al. Cutting Edge: beta-Catenin-
979 Interacting Tcf1 Isoforms Are Essential for Thymocyte Survival but Dispensable for
980 Thymic Maturation Transitions. *J Immunol.* 2017;198(9):3404-9.
981 39. Riley JL. PD-1 signaling in primary T cells. *Immunol Rev.* 2009;229(1):114-25.
982 40. Fife BT, and Pauken KE. The role of the PD-1 pathway in autoimmunity and peripheral
983 tolerance. *Ann N Y Acad Sci.* 2011;1217:45-59.
984 41. Francisco LM, Sage PT, and Sharpe AH. The PD-1 pathway in tolerance and
985 autoimmunity. *Immunol Rev.* 2010;236:219-42.
986 42. Diskin B, Adam S, Cassini MF, Sanchez G, Liria M, Aykut B, et al. PD-L1 engagement on T
987 cells promotes self-tolerance and suppression of neighboring macrophages and effector
988 T cells in cancer. *Nat Immunol.* 2020;21(4):442-54.
989 43. Walker LS, and Sansom DM. Confusing signals: recent progress in CTLA-4 biology. *Trends*
990 *Immunol.* 2015;36(2):63-70.
991 44. Im SJ, Hashimoto M, Gerner MY, Lee J, Kissick HT, Burger MC, et al. Defining CD8+ T cells
992 that provide the proliferative burst after PD-1 therapy. *Nature.* 2016;537(7620):417-21.
993 45. https://link.springer.com/article/10.1007/s11515-017-1445-3
994 46. Yu S, Zhou X, Steinke FC, Liu C, Chen SC, Zagorodna O, et al. The TCF-1 and LEF-1
995 transcription factors have cooperative and opposing roles in T cell development and
996 malignancy. *Immunity.* 2012;37(5):813-26.
997 47. https://link.springer.com/article/10.1007/s11515-017-1445-3
998 48. Fu J, Wu Y, Nguyen H, Heinrichs J, Schutt S, Liu Y, et al. T-bet Promotes Acute Graft-
999 versus-Host Disease by Regulating Recipient Hematopoietic Cells in Mice. *J Immunol.*
1000 2016;196(7):3168-79.
1001 49. Lord GM, Rao RM, Choe H, Sullivan BM, Lichtman AH, Luscinskas FW, et al. T-bet is
1002 required for optimal proinflammatory CD4+ T-cell trafficking. *Blood.* 2005;106(10):3432-
1003 9.
1004 50. Pearce EL, Mullen AC, Martins GA, Krawczyk CM, Hutchins AS, Zediak VP, et al. Control
1005 of effector CD8+ T cell function by the transcription factor Eomesodermin. *Science.*

1006 2003;302(5647):1041-3.
1007 51. Chen Y, Yu M, Zheng Y, Fu G, Xin G, Zhu W, et al. CXCR5(+)PD-1(+) follicular helper CD8 T
1008 cells control B cell tolerance. *Nat Commun.* 2019;10(1):4415.
1009 52. https://link.springer.com/article/10.1007/s11515-017-1445-3
1010 53. http://surgpathcriteria.stanford.edu/transplant/skinacutegvhd/printable.html
1011 54. http://surgpathcriteria.stanford.edu/transplant/giacutegvhd/printable.html

1012

1013
1014
1015
1016
1017
1018
1019
1020
1021
1022
1023
1024

1025

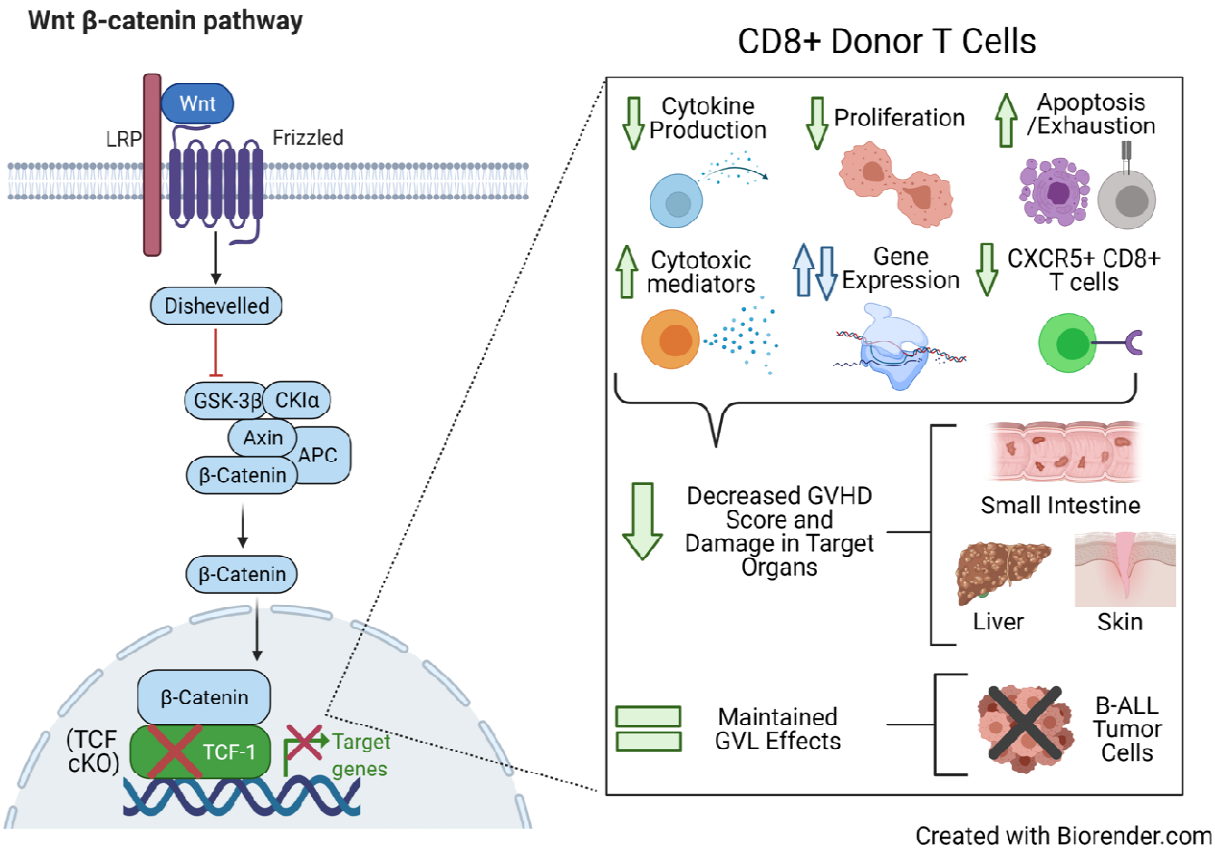

Summary Figure: TCF-1 separates GVHD from GVL by regulating mature alloactivated CD8 T cells. T Cell Factor-1 (TCF-1) is a T cell transcription factor involved in the Wnt pathway. Conditional deletion of TCF-1 in T cells led to reduced GVHD, yet maintained GVL effects again B-cell acute lymphoblastic leukemia (B-ALL) tumor cells. This occurred primarily due to: reduced cytokine production and proliferation; increased apoptosis, exhaustion, and production of cytotoxic mediators; and altered gene expression. The observed reduction in CXCR5+ CD8+ T cells may also have contributed to the reduced GVHD severity. These alterations led to reduced damage to target organs (liver, skin, and small intestine), yet the CD8 T cells were still able to clear tumor cells.

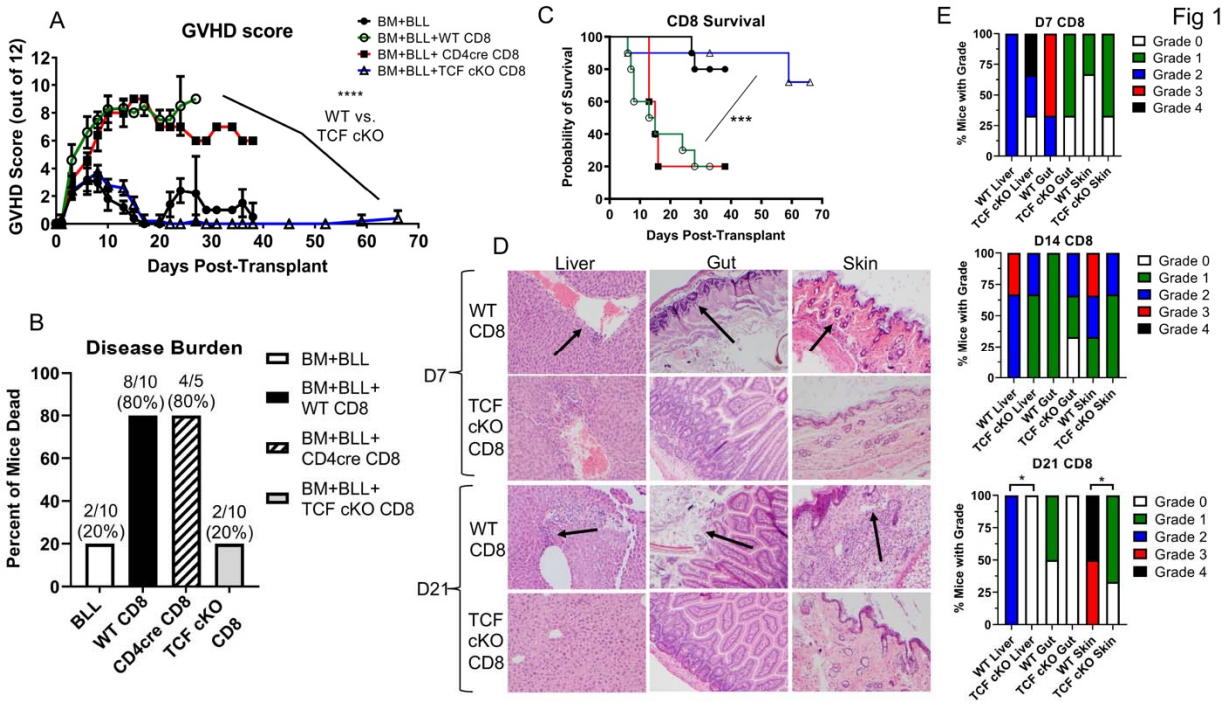

Figure 1: Loss of TCF-1 in donor CD8 T cells reduces severity and persistence of GVHD symptoms. BALB/c recipient mice (MHC haplotype D) were lethally irradiated and allotransplanted with $1X10^6$ CD8 T cells from WT, CD4cre, or TCF cKO donor mice (MHC haplotype b), as well as $10X10^6$ T cell-depleted bone marrow cells (BM) from BALB/c mice (MHC haplotype d). Recipient mice were also given $2X10^5$ luciferase-expressing B-ALL tumor cells (10, 40). **(A)** The recipient mice were given a GVHD clinical score three times per week until day 66, based on combined scores of fur texture, activity level, weight loss, posture, skin integrity, and diarrhea. Mean and SD are plotted, analyzed by two-way ANOVA. **(B)** Disease burden as determined by number of mice in each group that died by the end of the experiment. Percentage and number of mice listed above the bar for each group. **(C)** Survival for each group of recipient mice over the 66 days post-transplant, analyzed by Kaplan-Meier survival analysis. **(D)** At day 7, day 14, and day 21 post-transplant, organs were taken from recipient mice for histology analyses. Skin, liver, spleen, and small intestine were sectioned, stained with H&E, and

graded by a pathologist (A.M.) blinded to study conditions and slide groups. Representative sections for each organ per group and timepoint are shown. Arrows indicate tissue damage or lymphocyte infiltration. **(E)** Histology grades for each group of mice, shown as percentage of mice per group experiencing that grade. Grades 3-4 are considered severe GVHD, while grades 0-2 are considered mild GVHD. Data were analyzed by chi-square analysis. For all graphs, * means p-value ≤ 0.05, *** means p-value ≤ 0.001, and **** means p-value ≤ 0.0001. N=3-5 per group for **A-C** with one representative experiment shown, N=3 per group for **D-E**, one representative photo shown and summary data in **E.**

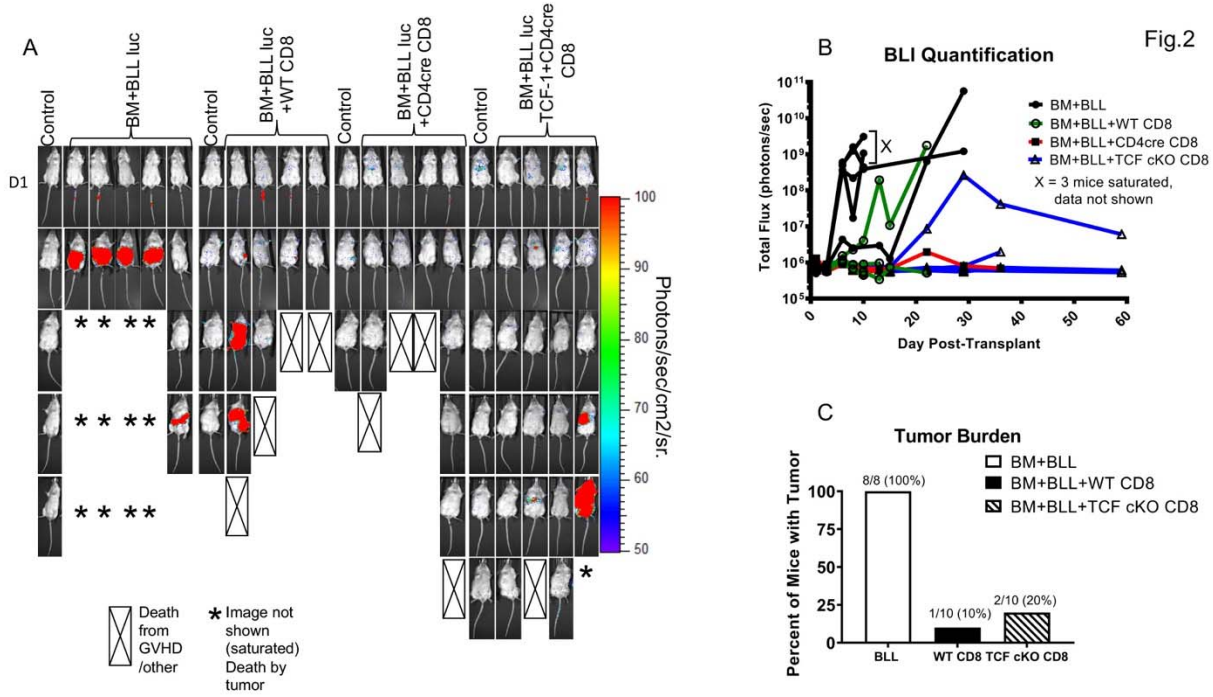

Figure 2: TCF-1-deficient CD8 T cells retain anti-tumor capabilities for the graft-versus-leukemia (GVL) effect. BALB/c mice were allotransplanted as in Fig. 1 with T cell-depleted BM and WT, CD4cre, or TCF cKO CD8 donor T cells, along with $2X10^5$ luciferase-expressing B-ALL tumor cells. Recipient mice were then injected with D-luciferin (i.p.) and imaged using the IVIS 200 imaging system. **(A)** Representative set of photos showing the tumor

bioluminescence and localization for transplanted groups. Control mice were untransplanted, BM+BLL mice received only BM and tumor cells, while the other groups received BM, tumor cells, and either WT, CD4cre, or TCF cKO donor CD8 T cells. Boxes with an "X" indicate death from GVHD or tumor, * indicates that the image was saturated due to excessively high signal, so the image is not shown. **(B)** Quantification of bioluminescence signal for each mouse in the transplanted groups for one representative experiment, as determined by total flux (photons per second). Note: 3 mice from the BM+BLL luc group in this experiment had saturated signals, so the data was excluded. **(C)** Tumor burden for tumor only, tumor with WT CD8, and tumor with TCF cKO CD8 groups, as determined by number/percentage of mice showing tumor bioluminescence and tumor presence at the end of the experiment. N=3-5 per group with one representative experiment shown.

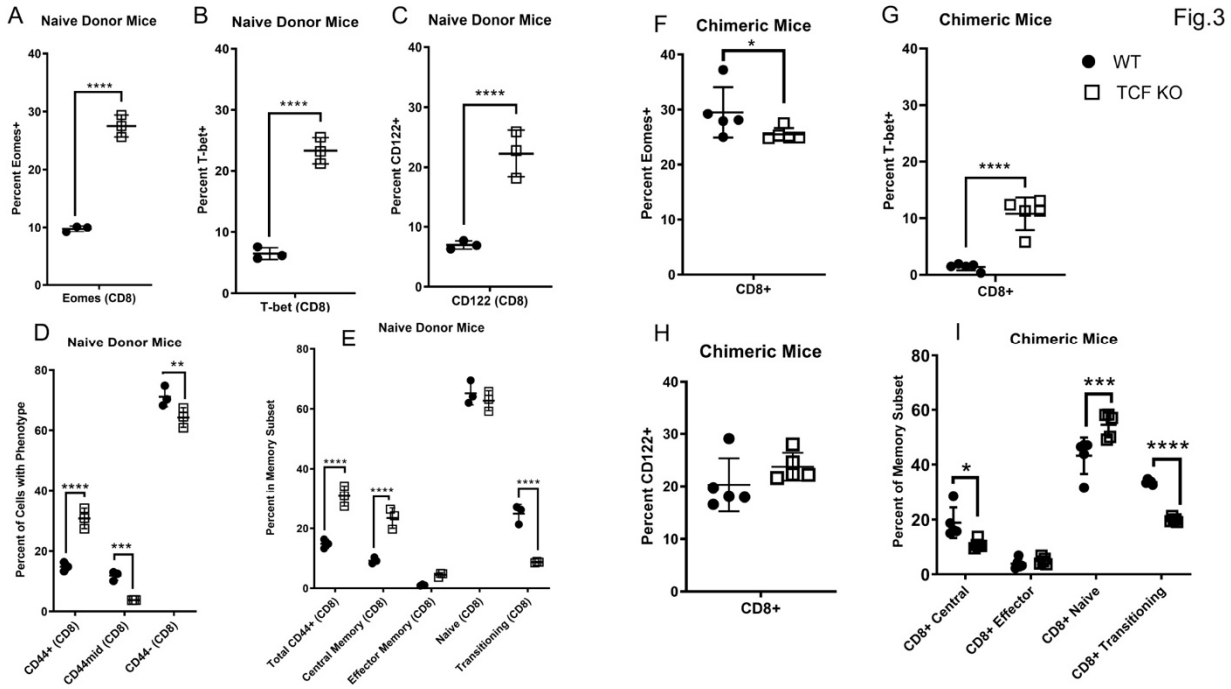

Figure 3: Loss of TCF-1 drives changes to mature CD8 T cell phenotype which are primarily cell-intrinsic. (A-E) Naive WT or TCF cKO donor mice were euthanized and

splenocytes were stained for flow cytometry phenotyping. **(A)** Percent of CD8 T cells expressing Eomes. **(B)** Percent of CD8 T cells expressing T-bet. **(C)** Percent of CD8 T cells expressing CD122. **(D)** Percent of CD8 T cells expressing CD44. **(E)** Percent of CD8 T cells expressing central memory, effector memory, transitioning/activating, or naive phenotypes. **(F-I)** Bone marrow chimeras were developed by lethally irradiating Thy1.1 mice and reconstituting with a 1:4 (WT:TCF cKO) mixture of bone marrow cells. Blood was tested at 9 weeks to ensure reconstitution with both donor cell types, and splenocytes were used at 10 weeks for phenotyping by flow cytometry. **(F)** Percentage of chimeric CD8 T cells expressing Eomes. **(G)** Percentage of chimeric CD8 T cells expressing T-bet. **(H)** Percentage of chimeric CD8 T cells expressing CD122. **(I)** Percentage of chimeric CD8 T cells expressing central memory, effector memory, naive, or transitioning/activating phenotypes. All data are plotted as individual points with mean and SD, all were analyzed with one-way or two-way ANOVA, or Student's t-test (depending on groups). For all graphs, * means p-value ≤ 0.05, *** means p-value ≤ 0.001, and **** means p-value ≤ 0.0001. For A-E, N=3 per group with one representative experiment shown, for F-I, N=5 with one experiment shown (done once).

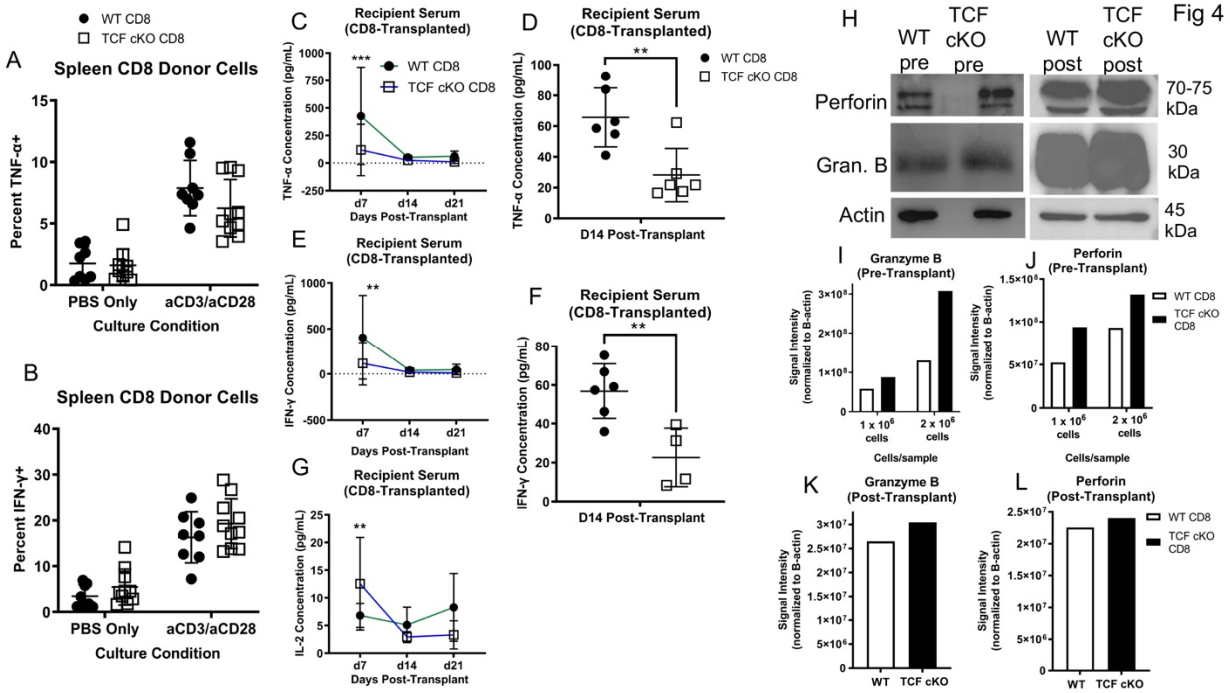

Figure 4: Loss of TCF-1 alters cytokine and cytotoxic mediator production by mature alloactivated CD8 T cells. (A-B) Recipient mice were allotransplanted with $1.5X10^6$ WT or TCF cKO donor CD3 T cells and BALB/c BM, as before. Splenocytes were taken at d7 post-transplant, restimulated by 6hr culture with Golgi Plug and PBS (control) or anti-CD3/anti-CD28 (TCR restim.), then stained for H2Kb, CD3, CD4, CD8, TNF-α, and IFN-γ. **(A)** TNF-α production and **(B)** IFN-γ production by donor CD8 T cells, as measured by percent cytokine-positive donor cells. For **A-B**, individual points are plotted with mean and SD shown. **(C-G)** At day 7, day 14, and day 21 post-transplant, serum was obtained from cardiac blood of allotransplanted recipient mice and tested for various cytokines using a LEGENDplex ELISA assay. **(C)** Serum levels (pg/mL) of TNF-α for WT and TCF cKO-transplanted mice over time and **(D)** at day 14 only. **(E)** Serum levels (pg/mL) of IFN-γ for WT and TCF cKO-transplanted mice over time and (F) at day 14 only. **(G)** Serum levels (pg/mL) of IL-2 over time for WT and TCF cKO-transplanted mice. For **C, E**, and **G**, means with SD are plotted, for **D** and **F**,

individual points with mean and SD are shown. All data in A-G were analyzed with Student's t-test or two-way ANOVA (depending on groups). ** means p-value ≤ 0.01, and *** means p-value ≤ 0.001. (H-L) Pre-transplant and post-transplant donor CD8 T cells were isolated from donors or WT- or TCF cKO-transplanted recipient spleens and lysed for Western blot. **(H)** Blot photos showing bands for perforin, Granzyme B, and actin. Protein levels normalized to B-actin for **(I)** Granzyme B in pre-transplant cells, **(J)** perforin in pre-transplant cells, **(K)** Granzyme B in post-transplant cells, and **(L)** perforin in post-transplant cells. N=3-5 per group for **A-B** with two experiments shown, n=5-6 per group for **C-G** with summary data (**C,E,G)** or points **(D,F)** shown from one representative experiment. **H-L** one well per condition as shown in blot, **I-L** one experiment plotted (done once).

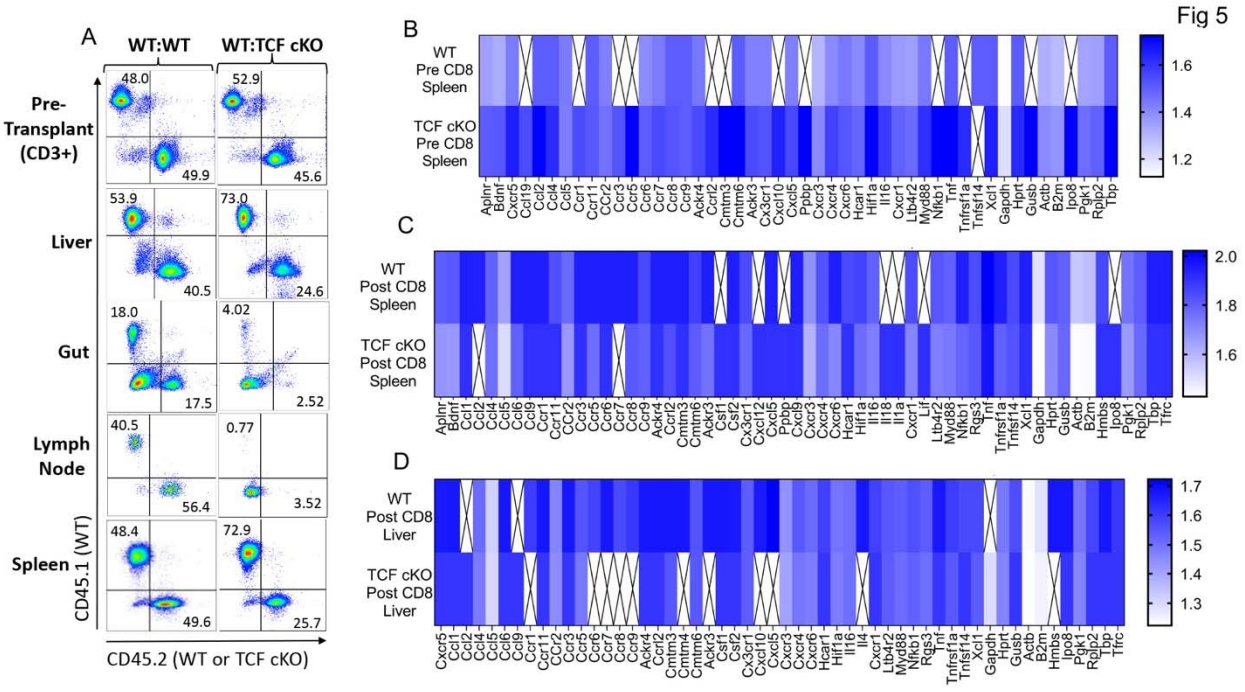

Figure 5: TCF-1 controls chemokine and chemokine receptor expression of donor CD8 T cells during alloactivation. As before, recipient BALB/c mice were allotransplanted with BALB/c BM and donor CD3 T cells from WT and TCF cKO mice. Here, the $1X10^6$ donor T

cells were a 1:1 mixture of WT (CD45.1):WT (CD45.2) or WT (CD45.1):TCF cKO (CD45.2) CD3 T cells. **(A)** Pre-transplant, a sample of donor cells was checked to ensure a 1:1 ratio of CD4 to CD8 T cells, and a 1:1 ratio of CD45.1:CD45.2 donor cells. At 7 days post-transplant, liver, gut, spleen, and lymph nodes were taken from euthanized recipient mice and processed to obtain lymphocytes. The lymphocytes were stained for H2Kb (donor cells), H2Kd (recipient cells), CD3, CD4, CD8, CD45.1, and CD45.2. Pre- and post-transplant flow plots from one representative recipient are shown here. **(B-D)** BALB/c mice were allotransplanted with BM and $1X10^6$ donor CD3 T cells from WT or TCF cKO mice (not mixed). Donor CD8 T cells were FACS-sorted from spleen of donors pre-transplant, and from spleen and liver of recipients at day 7 post-transplant. Cells were sorted into Trizol, then RNA was extracted using chloroform and converted to cDNA for qPCR analysis. cDNA was run on premade mouse chemokine/chemokine receptor assay plates, and results are displayed as heatmaps. Scales are shown at right, with fold change per gene compared to an 18S reference gene on each plate. White boxes with an "X" represent signals too low to detect or otherwise unreadable due to technical limitation/error. **(B)** Pre-transplant spleen donor CD8 T cells, **(C)** post-transplant spleen donor CD8 T cells, and **(D)** post-transplant liver donor CD8 T cells for WT versus TCF cKO donors. N=3 per group for A with one representative experiment shown, N=5 mice into one sample per condition for **B-D,** summary data shown.

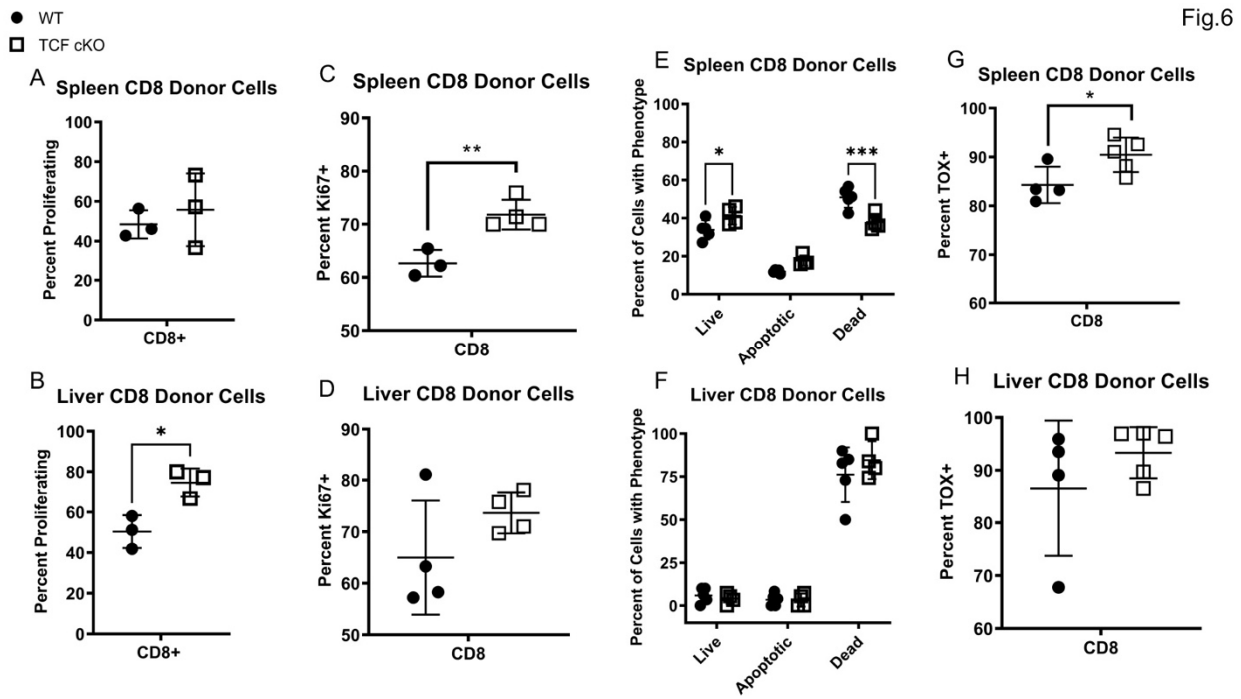

Figure 6: TCF-1 controls proliferation, apoptosis, and exhaustion of mature alloactivated CD8 T cells. (A-B) BALB/c mice were allotransplanted as before, with BALB/c BM and WT or TCF cKO CD3 donor T cells. Recipient mice were injected i.p. with 25mg/kg EdU in PBS on day 5 and 6 post-transplant. On day 7, spleen and liver were removed from recipients, processed to isolate lymphocytes, and stained with an EdU click chemistry staining kit to detect EdU. Cells were also stained for CD3, CD4, CD8, and H2Kb to identify donor cells. **(A)** Percent of donor cells proliferating by EdU+ in spleen, and **(B)** in liver. **(C-D)** In a similar experiment, splenic and liver-derived lymphocytes from allotransplanted recipient mice were stained for CD3, CD4, CD8, H2Kb, and Ki67 to identify proliferating/activated T cells. **(C)** Percent of donor CD8 cells proliferating by Ki67+ in spleen, and **(D)** in liver. **(E-F)** Recipient mice were allotransplanted as before with BM and WT or TCF cKO donor CD3 T cells. At day 7, spleen and liver were taken, processed to obtain lymphocytes, and stained for CD3, CD4, CD8, and H2Kb, and with Annexin V-FITC, and LIVE/DEAD Near-IR. Cells were divided into three populations: live (Ann.V-

NIR-), dead (Ann.V+ NIR+), or apoptotic (Ann.V+NIR-). This was done for **(E)** spleen and **(F)** liver. **(G-H)** As before, recipient mice were allotransplanted, and at day 7, spleen and liver were removed and processed to obtain lymphocytes. Lymphocytes were stained for H2Kb, CD3, CD4, CD8, and TOX to identify exhausted cells. This was done for **(G)** spleen and **(H)** liver. All data are shown as individual points with mean and SD, and were analyzed with Student's t-test or two-way ANOVA (depending on groups). * means p-value ≤ 0.05, ** means p-value ≤ 0.01, and *** means p-value ≤ 0.001. N=3-5 per group with one representative experiment shown.

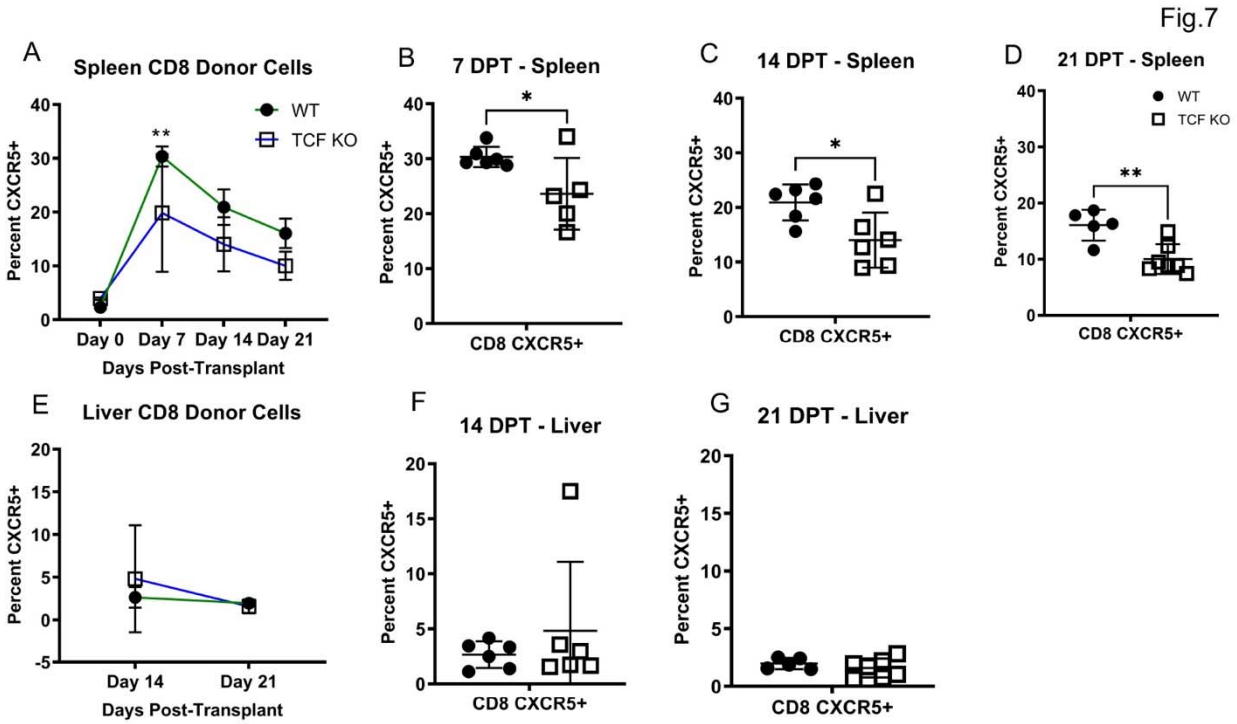

Figure 7: Reduced CXCR5 expression in CD8 T cells of TCF-1 deficient mice may contribute to reduced GVHD severity. Recipient BALB/c mice were allotransplanted with BALB/c BM and WT or TCF cKO donor CD8 T cells. Prior to transplant, a sample of donor cells was stained for CXCR5. At day 7, day 14, and day 21 post-transplant, spleen and liver were taken from recipient mice, processed to obtain lymphocytes, and stained for CD3, CD4, CD8, H2Kb, and CXCR5. **(A)** Expression of CXCR5 in spleen at day 0 and over time post-transplant.

(B-D) Expression of CXCR5 at each time point, **(B)** 7 days, **(C)** 14 days, and **(D)** 21 days post-transplant in the spleen. **(E)** Expression of CXCR5 in liver-derived donor cells over time post-transplant. **(F-G)** Expression of CXCR5 at **(F)** day 14 and **(G)** day 21 post-transplant in the liver. N=5-6 per group and condition, with summary data **(A,E)** or individual points **(B-D, F-G)** shown for one experiment (done once).

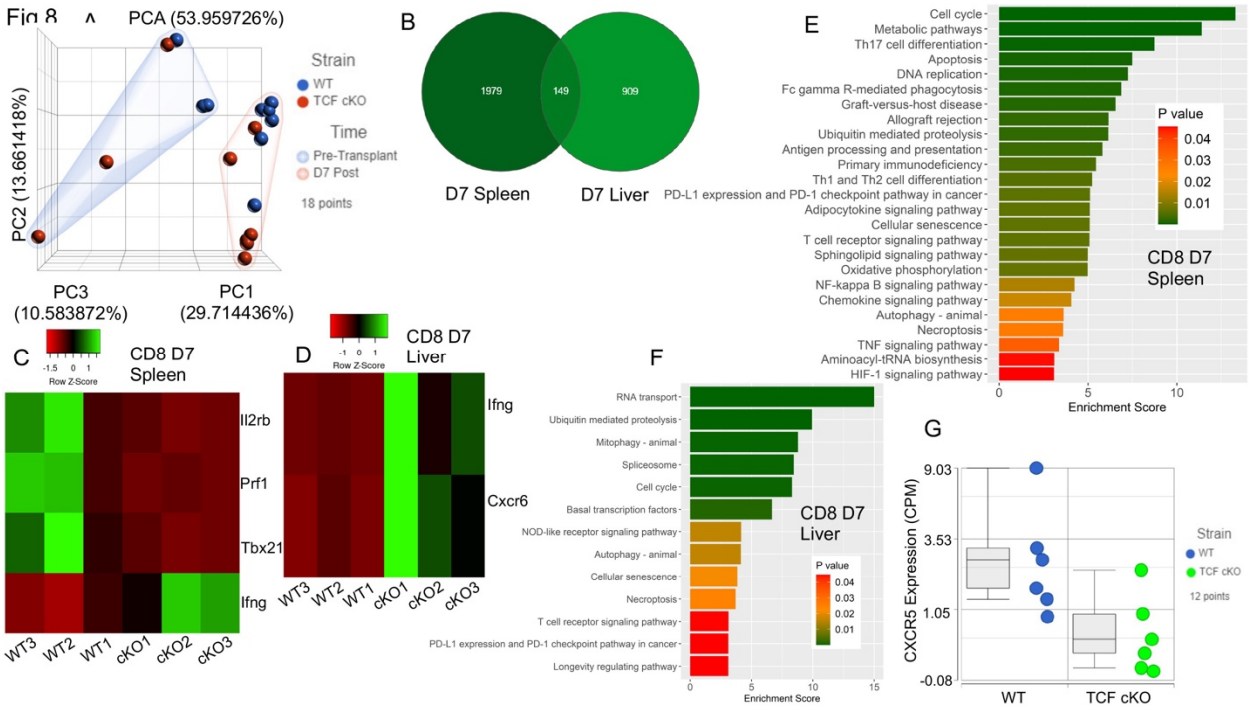

Figure 8: TCF-1 contributes to control of cell survival and immune signaling pathways in CD8 donor T cells. To perform RNA sequencing, recipient BALB/c mice were allotransplanted with BALB/c BM and WT or TCF cKO CD3 donor T cells. Pre-transplant CD8+ donor cells were FACS-sorted to obtain a sample for sequencing. At day 7 post-transplant, donor CD8 T cells were FACS-sorted back from spleen and liver of recipient mice. Cells were sorted into Trizol, then RNA was extracted and paired-end sequencing was performed. **(A)** PCA analysis showing clustering of donor CD8 T cells by strain and by timepoint (pre- and post-transplant). Points are colored by strain and grouped by timepoint. **(B)** Venn diagram showing number of

differentially expressed genes found in post-transplant spleen and liver for WT versus TCF cKO CD8 donor T cells. FDR ≤ 0.05 and fold change ≥ 2 or ≤ -2 were used as criteria for selection. **(C-D)** Heatmap showing select significantly changed genes in donor CD8 T cells from **(C)** post-transplant spleen, or **(D)** post-transplant liver. **(E-F)** Pathway enrichment analysis, with selected enriched pathways shown for **(E)** post-transplant liver and **(F)** post-transplant spleen. All pathways shown have p-value ≥ 0.05, and fill color indicates p-value. **(G)** Expression level of CXCR5 in counts per million reads for WT versus TCF cKO donor CD8 T cells, post-transplant, in spleen and liver. Individual samples are shown, with boxplot indicating summary statistics. Log scale is used on y-axis. N=3-5 samples per group and condition, one experiment shown (done once).

Supplemental Figure Legends:

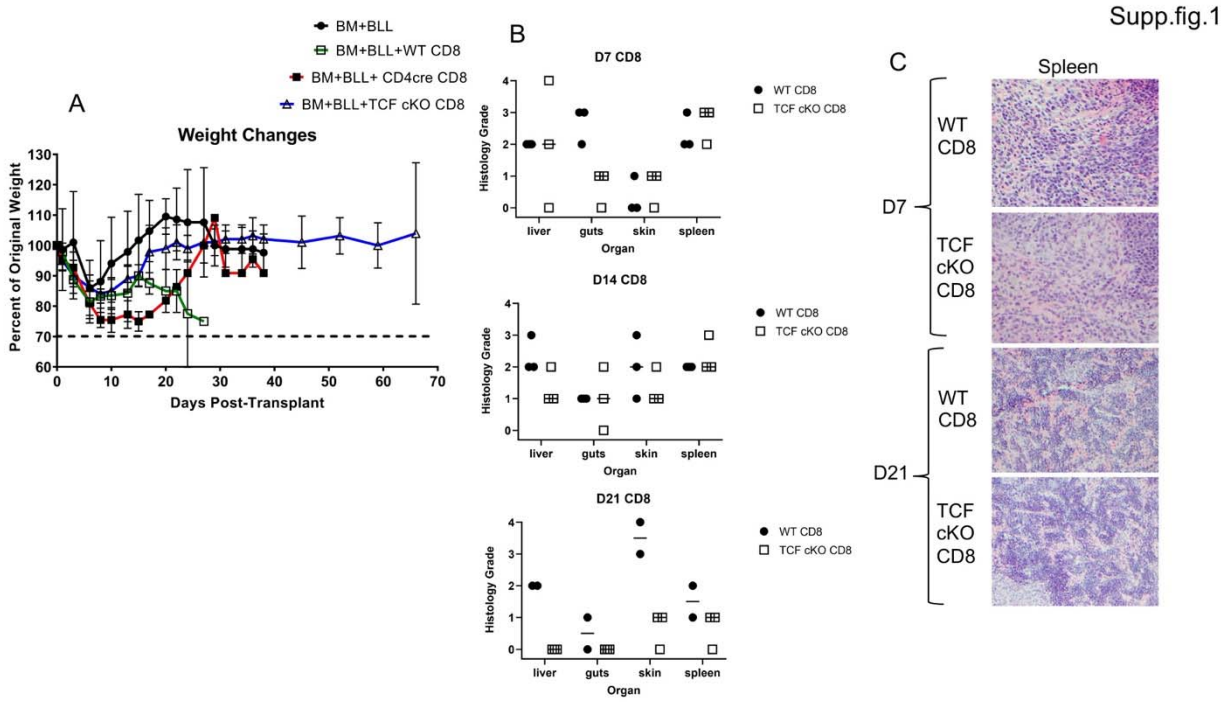

Supplemental Figure 1: GVHD symptoms and organ damage caused by donor CD8 T cells are reduced by loss of TCF-1, related to Figure 1. Recipient BALB/c mice were allotransplanted with BALB/c BM and WT, CD4cre, or TCF cKO CD8 T cells as described in Fig. 1. **(A)** Weight changes for each group of mice over the experiment, mean and SD are plotted. **(B)** GVHD histology score for organ sections (liver, spleen, skin, and small intestine) taken from recipient allotransplanted mice at day 7, day 14, and day 21 post-transplant. Sections were scored by a pathologist (A.M.) blinded to study conditions and slide identity. Individual points are plotted, with median shown. **(C)** Representative photos of spleen sections from day 7 and day 21 are shown. N=3-5 per group with one representative experiment shown in A, summary data with points in B, and one representative photo per strain/time in C.

Supp.fig.2

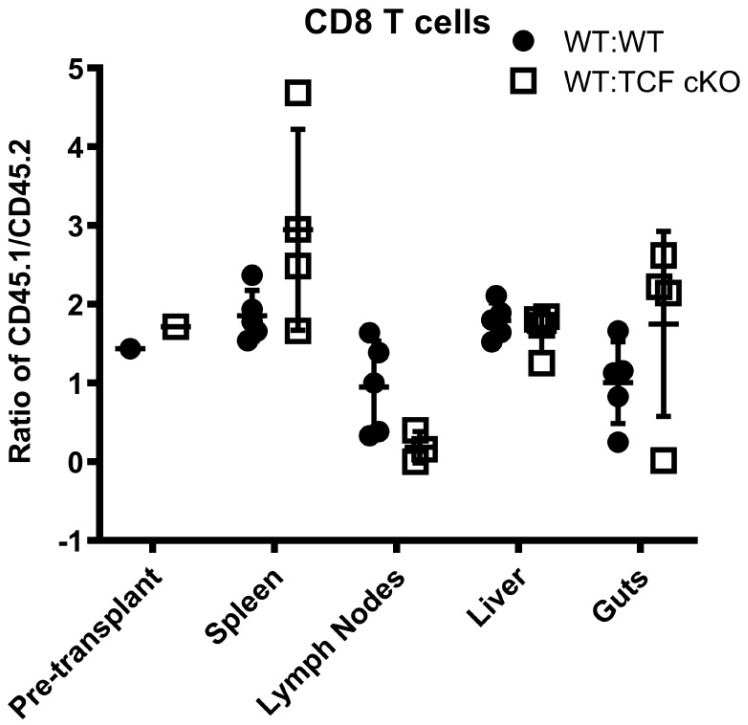

Supplemental Figure 2: Loss of TCF-1 does not significantly disrupt migration of CD8 T cells, related to Figure 5. Recipient BALB/c mice were allotransplanted with BALB/c BM and a 1:1 mixture of WT (CD45.1):WT (CD45.2) or WT (CD45.1):TCF cKO (CD45.2) donor CD3 T cells (total $1X10^6$ cells). Prior to transplant and at day 7 post-transplant, the ratio of CD45.1 to CD45.2 donor cells was assessed by flow cytometry. Pre-transplant samples were taken from cells to be transplanted, and day 7 samples were obtained from recipient spleen, lymph nodes, liver, and small intestine. Individual points are plotted, with mean and SD shown. Data were analyzed with two-way ANOVA. N=4-5 per group (n=1 for pre-transplant), one representative experiment shown.

Supp.fig.3

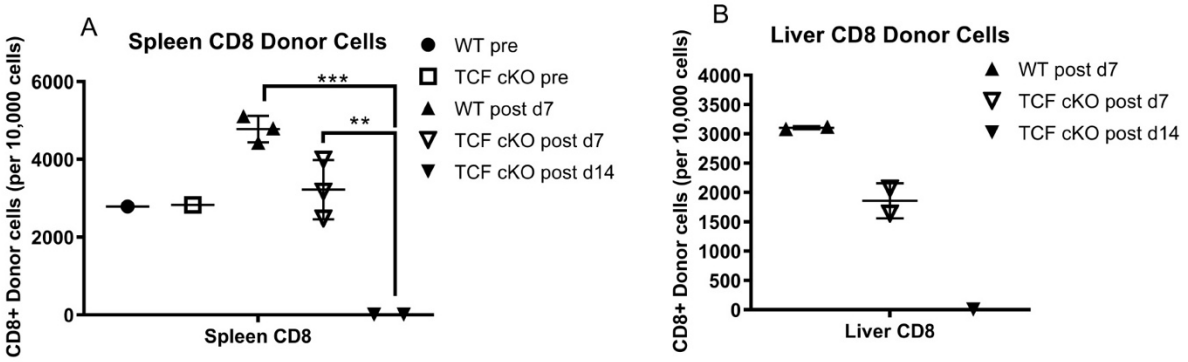

Supplemental Figure 3: Donor CD8 T cell numbers are reduced when TCF-1 is lost, related to Figure 6. Recipient mice were allotransplanted with BALB/c BM and WT or TCF cKO CD3 donor T cells. Donor CD8 T cells were FACS-sorted from pre-transplant donors or from recipient spleen and liver 7 days post-transplant. TCF cKO donor cells only were also sorted at day 14 from spleen and liver. Number of CD8+ donor cells obtained by sorting per 10,000 sorted cells is shown in **(A)** spleen and **(B)** liver. Individual points are shown with mean and SD, data were analyzed by two-way ANOVA. ** means p-value ≤ 0.01, and *** means p-value ≤ 0.001. N=2-3 per group (n=1 for pre-transplant), one representative experiment shown.

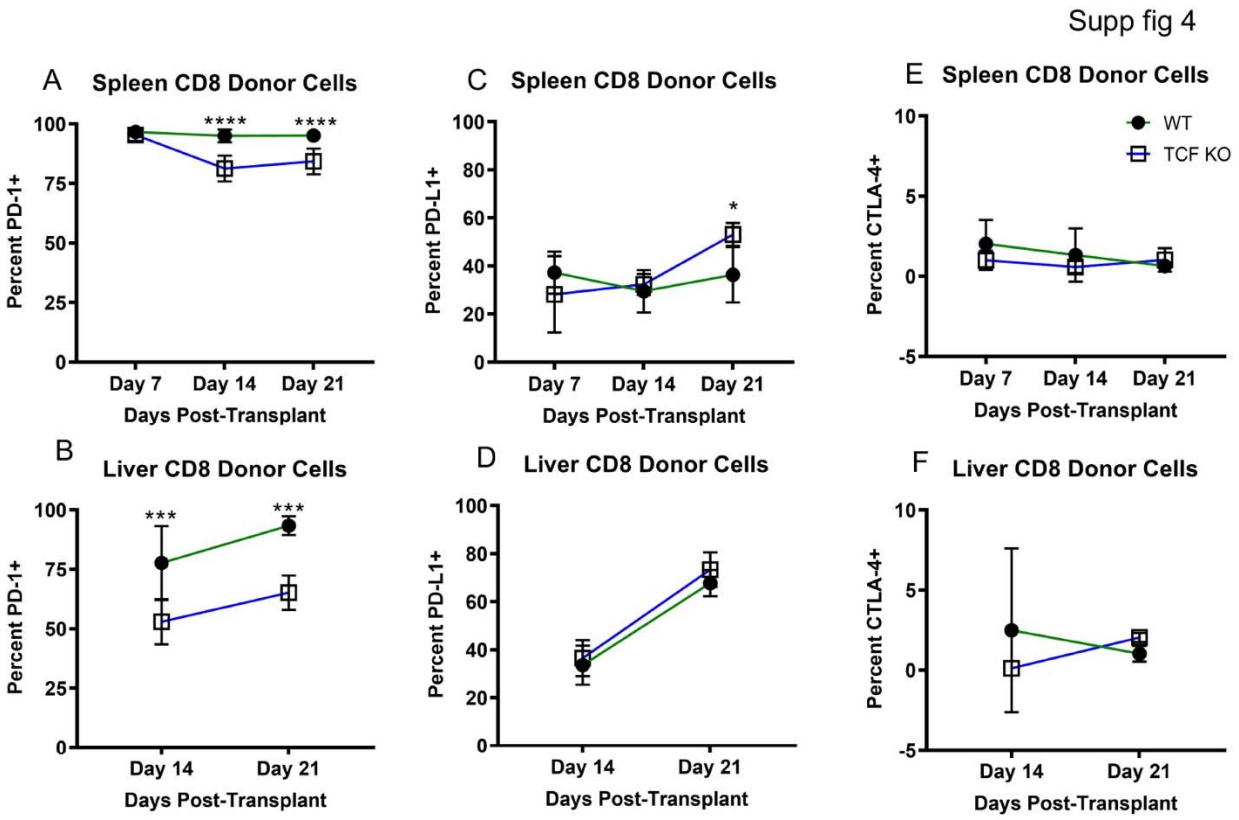

Supplemental Figure 4: Loss of TCF-1 changes the suppressive profile of CD8 donor T cells, related to Figure 6. Recipient BALB/c mice were allotransplanted with BALB/c BM and WT or TCF cKO donor CD8 T cells. At day 7, day 14, and day 21 post-transplant, spleen and liver were taken from recipients and processed to obtain lymphocytes. Lymphocyes were stained for CD3, CD4, CD8, H2Kb, PD-1, PD-L1, and CTLA-4. **(A)** Expression of PD-1 on CD8+ donor cells in spleen over time. **(B)** Expression of PD-1 on CD8+ donor cells in liver over time. **(C)** Expression of PD-L1 on CD8+ donor cells in spleen over time. **(D)** Expression of PD-L1 on CD8+ donor cells in liver over time. **(E)** Expression of CTLA-4 on CD8+ donor cells in spleen over time. **(F)** Expression of CTLA-4 on CD8+ donor cells in liver over time. Mean and SD are shown, data were analyzed with two-way ANOVA, * means p-value ≤ 0.05, *** means p-value

≤ 0.001, and **** means p-value ≤ 0.0001. N=3-4 per group and timepoint, summary data from one experiment shown (done once).

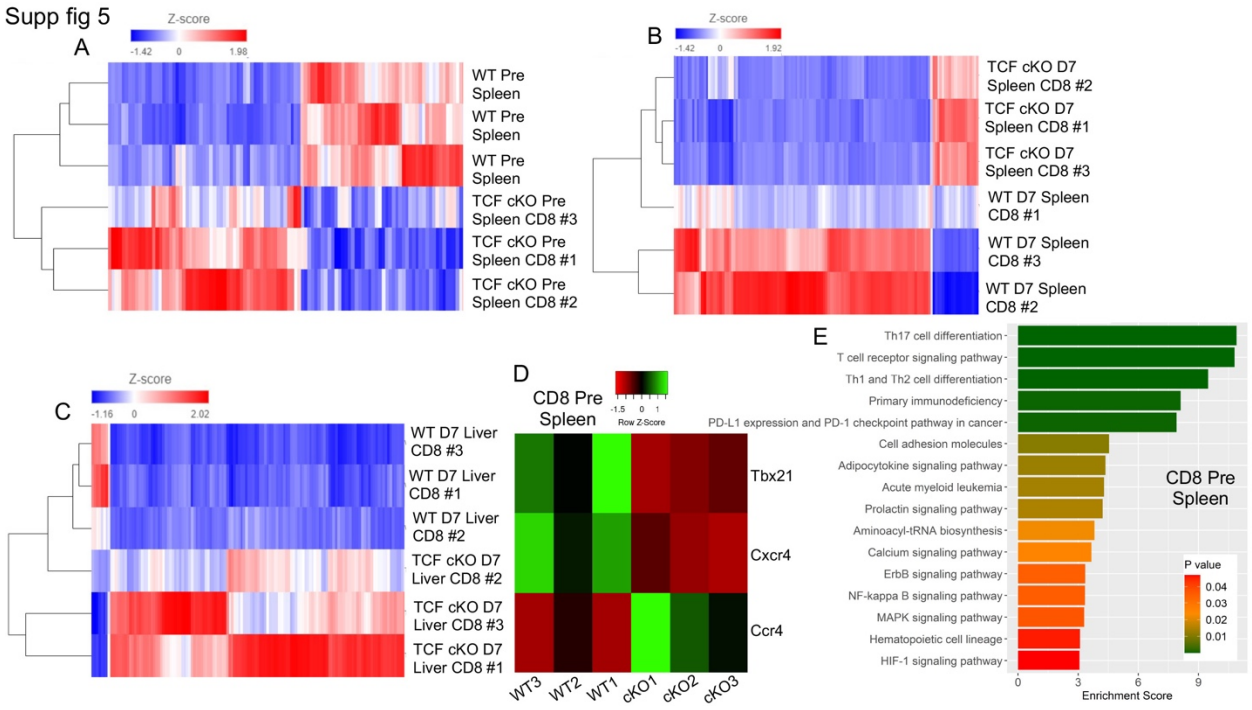

Supplemental Figure 5: Donor CD8 T cell samples cluster by strain, and TCF-1 alters pre-transplant gene expression, related to Figure 8. As for Fig. 8, recipient mice were allotransplanted with BM and WT or TCF cKO donor CD3 T cells. Pre- and day 7 post-transplant donor cells were FACS-sorted from donor spleen or recipient spleen/liver, respectively. RNA sequencing was performed on donor cells as in Fig. 8. **(A-C)** Hierarchical clustering was performed for **(A)** pre-transplant spleen, **(B)** post-transplant spleen, and **(C)** post-transplant liver samples. **(D)** Heatmap showing select significantly changed genes in donor CD8 T cells from pre-transplant spleen. **(E)** Pathway analysis was performed on pre-transplant CD8 donor T cell samples from spleen. Differentially expressed genes for **D-E** were identified by p-

value ≤ 0.05 (rather than FDR ≤ 0.05) and fold change ≥ 2 or ≤ -2. N=3 per group and condition, one experiment shown (done once).

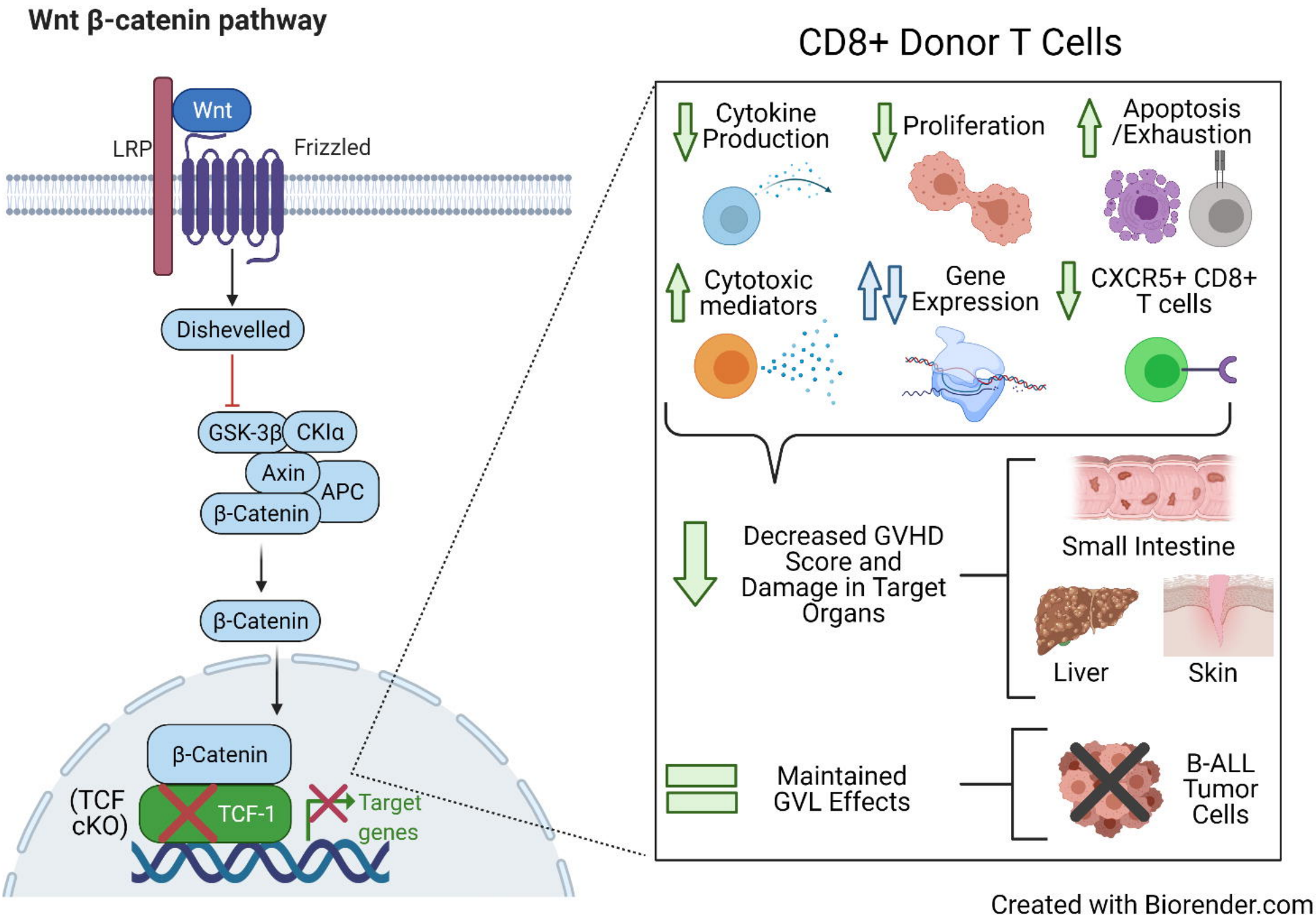
Wnt β-catenin pathway
Wnt
LRP
Frizzled
Dishevelled
GSK-3β
CKIα
Axin
APC
β-Catenin
β-Catenin
β-Catenin
(TCF cKO)
TCF-1
Target genes
CD8+ Donor T Cells
Cytokine Production
Proliferation
Apoptosis /Exhaustion
Cytotoxic mediators
Gene Expression
CXCR5+ CD8+ T cells
Decreased GVHD Score and Damage in Target Organs
Small Intestine
Liver
Skin
Maintained GVL Effects
B-ALL Tumor Cells
Created with Biorender.com